C.P. No. 1392

C.P. No. 1392

PROCUREMENT EXECUTIVE, MINISTRY OF DEFENCE

AERONAUTICAL RESEARCH COUNCIL

CURRENT PAPERS

Two-Dimensional Aerofoils and Control Surfaces in Simple Harmonic Motion in Incompressible Inviscid Flow

- by -

B.C. Basu and G.J. Hancock

Department of Aeronautical Engineering

Queen Mary College, London

LONDON: HER MAJESTY'S STATIONERY OFFICE

1978

£3 net

C.P. No.1392*
September 1976

TWO-DIMENSIONAL AEROFOILS AND CONTROL SURFACES IN SIMPLE HARMONIC MOTION IN INCOMPRESSIBLE INVISCID FLOW

- by -
B.C. Basu and G.J. Hancock

SUMMARY

A numerical method based on the A.M.O. Smith technique has been developed for the calculation of the two-dimensional potential flow about an aerofoil of arbitrary shape undergoing small amplitude simple harmonic motions. Problems considered include aerofoils oscillating in pitch, aerofoils oscillating in heave, aerofoils in harmonic travelling gusts and control surface oscillations. Comparison with analytic solutions, where available, is good.

Significant differences between linear and non-linear theory are shown especially for the in-phase hinge moment coefficients.

*Replaces ARC.37 204

NOTATION

x, z	co-ordinates measured along and normal to the chord line of the aerofoil.
α	aerofoil incidence
δ	control surface deflection
U_∞	free stream velocity
ρ	density
c_p	pressure coefficient
c	chord length
$C_L = \frac{\text{Lift}}{\frac{1}{2}\rho U_\infty^2 c}$	
$C_M = \frac{\text{Moment}}{\frac{1}{2}\rho U_\infty^2 c^2}$	
$C_H = \frac{\text{Hinge Moment}}{\frac{1}{2}\rho U_\infty^2 c^2}$	
Γ	circulation
γ	vorticity
u, w	perturbation velocity components along x and z axis
σ	body surface source strength
ω	frequency of oscillation
ϕ	velocity potential
$\nu(=\omega c/U_\infty)$	frequency parameter
$\zeta_s(x)$	steady aerofoil contour
$\bar{x}$, $\bar{z}$	non-dimensional co-ordinate relative to the chord
Δ_i	element length
θ	angle of pitch
h	ordinate of the heaving motion
A_{ji}, B_{ji}	influence coefficients
C_i, S_i	tabulated functions

Subscripts

s	steady state condition
o	oscillatory condition
w	wake
u	upper surface
ℓ	lower surface
g	gust

1. INTRODUCTION

A.M.O. Smith and his co-workers[1] have developed an 'exact' numerical method for the solution of the flow characteristics around a stationary body immersed in a uniform inviscid incompressible stream. Originally the method was applied to calculate the flow about axi-symmetric bodies at zero incidence and plane flow about two dimensional non-lifting and lifting aerofoils. Later the method was extended to handle cross flows about axi-symmetric bodies[2] and subsequently to deal with three dimensional flows[3].

For a steady two dimensional lifting aerofoil the basic concept is to replace the aerofoil surface by a number of straight line elements on which are placed uniform source and vorticity distributions; the uniform source strength on each element varies from element to element, but the strength of the uniform vorticity distribution over each element is the same for all elements. The strengths of the source distributions and vorticity distributions are determined from the boundary condition of tangential flow at the mid point of each element together with the Kutta condition of equal pressures at the mid points of the two elements either side of the trailing edge.

Extensions of the A.M.O. Smith technique to two dimensional unsteady aerofoil problems are described by Giesing[4,5]. For a completely general unsteady motion of a two dimensional aerofoil starting at time $t = 0$ Giesing[4] developed a numerical technique in which the flow characteristics are determined at successive time increments, the non-linear rolled up wake pattern then evolves naturally in the solution. For many practical problems, for example those associated with flutter and response to turbulence, interest is limited to an aerofoil oscillating at a small amplitude in simple harmonic motion; Giesing[5] developed a simplified numerical procedure for such oscillatory motions.

Analytical solutions for two dimensional oscillating aerofoils have been developed by Küssner and Von Gorup[6], Van de Vooren and Van de Vel[7] and Hewson-Browne[8] - all based on transformation techniques. Although these solutions have a limited practical application because of their restriction to particular aerofoil geometries such solutions are valuable as standard results for comparison with results from more approximate numerical methods. The solution by Van de Vooren and Van de Vel[7] is particularly useful because it gives detailed pressure distributions while the other two[6,8] give only the overall force and moment coefficients.

In this paper a numerical technique is developed for a two dimensional aerofoil performing harmonic variations about an arbitrary mean incidence, but limited to small amplitudes of perturbation. The method is similar in principle to that of Giesing[5] but some modifications have been introduced. The main modification is the application of a different Kutta condition.

In the present method incremental oscillatory source and vortex distributions are superimposed on the steady source and vortex distributions on elements distributed over the mean steady profile, and an oscillatory vortex distribution, representing the shed vorticity due to the rate of change of circulation, is placed on the mean streamline from the trailing edge. It is further assumed that the shed trailing vortex sheet is convected downstream with the free stream velocity. The unsteady boundary conditions are satisfied on the mean profile. It is anticipated that these approximations, which introduce considerable simplification to the numerical work, will be reasonable for small amplitudes of oscillation.

The formulation of the trailing edge Kutta condition in two dimensional unsteady flow presents some difficulty. If a Kutta condition is stipulated as the condition that the flow separates from the trailing

edge, which is implied when the total tangential velocities in the downstream direction on the upper and lower surface at the trailing edge are finite, then it follows from the unsteady Bernoulli equation that in general there is a discontinuity in pressure at the trailing edge of the aerofoil. If on the other hand a Kutta condition is stipulated as the condition of zero loading at the trailing edge then it does not follow that the flow will necessarily separate at the trailing edge. Exactly what happens in physical reality is not yet clear but until further evidence is forthcoming it has been suggested[9] that in general two Kutta conditions are necessary to obtain results which represent the physical flow for unsteady aerofoil motions, namely that the flow must separate from the trailing edge and that the loading at the trailing edge must be zero.

In the formulation of the unsteady theory which is linearised in the amplitude of perturbation, the velocity of convection of the shed vorticity needs to be assumed, in the present paper the velocity of convection is taken to be the free stream velocity. Thus to find a unique value of the aerofoil circulation, Γ, at any time t, one Kutta condition at the trailing edge is sufficient. Giesing[5] applied the condition of flow separation at the trailing edge by equating the tangential velocities on the upper and lower surfaces close to the trailing edge in the downstream directions, without reference to the zero load condition. In this paper the velocity condition at the trailing edge is not used, instead the Kutta condition is taken to be equality of the pressures on the upper and lower surface in the neighbourhood of the trailing edge.

In the analytic solution of Van de Vooren and Van de Vel[7] the Kutta condition is a hybrid one; the Kutta condition is stipulated in the transformed circle plane and the point on the circle corresponding to the trailing edge in the physical plane is made a stagnation point. This Kutta condition satisfies zero loading and smooth flow at the

trailing edge only when the trailing edge is a cusp. For a non-zero trailing edge angle this Kutta condition gives an infinite velocity associated with a weak singularity, together with a small finite loading at the trailing edge.

The numerical method described in this paper has been applied to the particular symmetrical aerofoil studied by Van de Vooren and Van de Vel[7] undergoing pitching oscillations. The numerical results for the in-phase and out-of-phase pressure distributions agree well with the analytic solution of Van de Vooren and Van de Val.

Numerical results have been obtained for a symmetrical and an 8.6% cambered Karman-Trefftz aerofoil pitching about the mid chord at mean angles of 0° and 10° incidences. Comparison of the present method with linearised theory shows some differences in pressure distributions, and in the lift and moment coefficients. Mean angle of incidence can affect the lift and moment coefficients. Camber has little effect on the lift and moment coefficients when the mean angle of incidence is 0° but a more substantial effect when the mean angle of incidence is 10°.

An 8.4% thick symmetrical Von Mises aerofoil has been investigated for heaving oscillations at 0° mean incidence. Comparison with linearised theory shows that linearised theory overestimates somewhat the lift and moment coefficients, both in- and out-of-phase components, for all values of frequency parameter.

The present method has also been applied to the case of an aerofoil proceeding through a sinusoidal vertical gust. The particular aerofoil is an 8.4% thick symmetrical Von Mises aerofoil. Comparison with linearised theory shows that, for values of frequency parameter up to about unity, the difference between the linearised solution and the solution of the present method is small. For frequency parameters greater than unity

the difference is still small for the out-of-phase components of the lift and moment coefficients, but the difference increases progressively with the frequency parameter for the in-phase components of these coefficients.

The aerodynamic characteristics induced by a control surface oscillating about its hinge line have been calculated for a symmetrical and a cambered (8.6%) Karman-Trefftz aerofoil section with a control surface of 30% chord. The difference in the lift and moment coefficients, both in- and out-of-phase components, compared with results from linearised theory, can be significant but the difference in the in-phase component of the hinge moment coefficient is especially large. Aerofoil mean incidence does not seriously affect the lift and moment coefficients, both in- and out-of-phase components, or the out-of-phase component of the hinge moment coefficients although there is some difference on the in-phase hinge moment coefficients. Camber affects slightly the lift, moment and hinge moment coefficients, the effect is especially noticeable for the in-phase components of the hinge moments. There appears to be no effect of mean control surface angle.

2. MATHEMATICAL FORMULATION FOR PITCHING OSCILLATION

The problem is to determine the pressure distribution, total force and moment on an aerofoil oscillating in a steady incompressible inviscid flow as shown in Fig. 1.

Cartesian co-ordinates (x,z) are taken with the origin coinciding with the point about which the aerofoil oscillates in simple harmonic motion. It is assumed that the axis of oscillation lies on the chord line. The free stream velocity U_∞ is inclined at the angle of incidence of α to the Ox axis as shown in Fig. 1.

The equation of the steady aerofoil profile relative to the axis system is denoted by

$$\left.\begin{aligned} z &= \zeta_{s_u}(x) \quad \text{On upper surface} \\ &= \zeta_{s_\ell}(x) \quad \text{On lower surface} \end{aligned}\right\} . \tag{1}$$

In the case of a symmetrical profile

$$\zeta_{s_u}(x) = -\zeta_{s_\ell}(x) . \tag{2}$$

The simple harmonic motion of the aerofoil to be superimposed on the steady profile, given by eqn. (1), is denoted by

$$\theta = \theta_0 e^{i\omega t} , \tag{3}$$

where ω is the frequency and θ_0 is the amplitude of oscillation.

Since the flow exterior to the aerofoil and wake is irrotational the total perturbation velocity components u and w are derived from a perturbation velocity potential ϕ such that

$$\begin{aligned} u &= \frac{\partial \phi}{\partial x} , \\ w &= \frac{\partial \phi}{\partial z} . \end{aligned} \tag{4}$$

Substitution of eqn. (4) into the equation of continuity gives

$$\frac{\partial^2 \phi}{\partial x^2} + \frac{\partial^2 \phi}{\partial z^2} = 0. \tag{5}$$

The equations of motion can be expressed in terms of the unsteady Bernoulli equation namely

$$p + \tfrac{1}{2}\rho[(U_\infty \cos\alpha + u)^2 + (U_\infty \sin\alpha + w)^2] + \rho\frac{\partial \phi}{\partial t} = \text{constant} . \tag{6}$$

The Laplace equation (5) and Bernoulli equation (6) are the basic equations governing the fluid motion and pressure respectively.

The unsteady aerofoil motion will induce an oscillatory circulation around the aerofoil. In order to preserve the overall conservation of vorticity any change in circulation around the aerofoil must cause vorticity to be shed and convected into the wake.

2.1 BOUNDARY CONDITION

If u_s and w_s are the steady perturbation velocity components on the aerofoil surface the steady boundary condition of tangency of flow can be written

$$\left.\begin{aligned}(U_\infty \sin\alpha + w_s) &= (U_\infty \cos\alpha + u_s)\zeta'_{s_u}(x) \text{ on upper surface} \\ &= (U_\infty \cos\alpha + u_s)\zeta'_{s_\ell}(x) \text{ on lower surface}\end{aligned}\right\}, \tag{7}$$

where the dash denotes differentiation with respect to x.

Normalising eqn. (7) with respect to U_∞ then

$$\left.\begin{aligned}(\sin\alpha + \bar{w}_s) &= (\cos\alpha + \bar{u}_s)\,\zeta'_{s_u}(x) \text{ on upper surface} \\ &= (\cos\alpha + \bar{u}_s)\,\zeta'_{s_\ell}(x) \text{ on lower surface}\end{aligned}\right\}, \tag{8}$$

where $\bar{u}_s$ and $\bar{w}_s$ are the normalised perturbation velocity components.

When the aerofoil oscillates in simple harmonic motion the point (X,Z) on the aerofoil at any instant t, defined in terms of fixed axes, may be defined as

$$\left.\begin{aligned}X &= x_s + \zeta_{s_u}(x_s)\theta_o e^{i\omega t} \quad \text{on upper surface} \\ &= x_s + \zeta_{s_\ell}(x_s)\theta_o e^{i\omega t} \quad \text{on lower surface} \\ Z &= \zeta_{s_u}(x_s) - x_s\theta_o e^{i\omega t} \quad \text{on upper surface} \\ &= \zeta_{s_\ell}(x_s) - x_s\theta_o e^{i\omega t} \quad \text{on lower surface}\end{aligned}\right\}, \tag{9}$$

where θ_o is assumed to be small, and x_s, ζ_s refer to a point on the mean profile.

The boundary condition for the oscillating aerofoil can be written as

$$\frac{U_\infty \sin\alpha + w - \partial Z/\partial t}{U_\infty \cos\alpha + u - \partial X/\partial t} = \left(\frac{\partial Z}{\partial X}\right)_{t=\text{const}} = \frac{\partial Z/\partial x_s}{\partial X/\partial x_s}, \tag{10}$$

where u and w are the total perturbation velocities at the surface of the aerofoil relative to still air, and $\partial Z/\partial t$ and $\partial X/\partial t$ are the surface

velocities in the z and x directions respectively. Thus at any point on the aerofoil surface the ratio of the total velocities in the z and x directions relative to the aerofoil surface is equal to the instantaneous slope at that point.

The boundary condition eqn. (10) should strictly be applied on the moving aerofoil surface (X,Z), however, for the present calculations, this boundary condition is applied on the stationary mean aerofoil surface, (x_s, ζ_s). It is anticipated that the errors will be small for small amplitudes θ_o.

It is now assumed that the response variables will be composed of an oscillatory solution superimposed on the basic steady solution. The effect of any higher harmonics is neglected because it is expected that the magnitude of these higher harmonics will be small. Thus

$$\begin{aligned} u &= u_s + u_o e^{i\omega t} , \\ w &= w_s + w_o e^{i\omega t} , \\ \phi &= \phi_s + \phi_o e^{i\omega t} . \end{aligned} \tag{11}$$

From eqns. (9), (10) and (11) the following relations are obtained for the upper surface

$$\sin\alpha + \bar{w}_s = (\cos\alpha + \bar{u}_s)\, \bar{\zeta}'_{s_u}(\bar{x}) , \tag{12}$$

and

$$\bar{w}_o - \bar{u}_o\, \bar{\zeta}'_{s_u}(\bar{x}) = -\theta_o\{(\cos\alpha + \bar{u}_s) + (\sin\alpha + \bar{w}_s)\, \bar{\zeta}'_{s_u}(\bar{x}) + i\nu(\bar{x} + \bar{\zeta}_{s_u}(\bar{x})\, \bar{\zeta}'_{s_u}(\bar{x}))\} , \tag{13}$$

where $\bar{u}_s$, $\bar{w}_s$, $\bar{u}_o$, $\bar{w}_o$ are normalised perturbation velocities, $\bar{x}(= \frac{x}{c})$, $\bar{\zeta}_{s_u}$ $(= \zeta_{s_u}/c)$ are non dimensional co-ordinates, and ν is the non dimensional frequency parameter $(\omega c/U_\infty)$.

Similar relations can be written down for the lower surface.

Eqn. (12) is the steady boundary condition while eqn. (13) may be considered as the incremental unsteady boundary conditions relating $\bar{u}_o$ and $\bar{w}_o$. It can be seen that the boundary condition for $\bar{u}_o$ and $\bar{w}_o$, eqn. (15), involves the steady distributions $\bar{u}_s$ and $\bar{w}_s$.

When the frequency of oscillation tends to zero the boundary condition eqn. (15) becomes

$$\bar{w}_o - \bar{u}_o \bar{\zeta}_{s_u}(\bar{x}) = -\theta_o\{(\cos\alpha + \bar{u}_s) + (\sin\alpha + \bar{w}_s)\,\bar{\zeta}'_{s_u}(\bar{x})\} . \qquad (14)$$

Eqn. (16) may be regarded as the approximate boundary condition for the incremental problem of a steady aerofoil when the incidence is increased from α_s to $(\alpha_s + \theta_o)$. The exact steady state solution at $(\alpha_s + \theta_o)$ can be obtained by satisfying the exact boundary condition. A comparison of these two steady solutions has shown that the error in the approximate method, using eqn. (14), is of the order of 0.5% for a symmetrical aerofoil with θ_o up to 5°. It is, therefore, anticipated that the present numerical method is sufficiently accurate for amplitudes of oscillation of up to 5°.

2.2 WAKE FLOW

According to Kelvin's circulation theorem the total circulation around a circuit in irrotational flow must be zero. Thus any change in circulation around the aerofoil must show up as shed vorticity in the wake. When the aerofoil oscillates the unsteady component of the circulation around the aerofoil $\Gamma_o e^{i\omega t}$ changes with time. Hence an oscillating aerofoil must always shed vorticity in the wake. It is assumed that this shed vorticity is convected along the steady trailing streamline as shown in Fig. 2; this approximation is consistent with a theory which is linearised in amplitude of oscillation.

In the present approach it is also assumed that the vortex sheet is convected with the flow at the free stream velocity. This assumption is expected to be reasonable for most of the wake with the possible

exception of a small region just aft of the trailing edge. It is anticipated however that this approximation, which simplifies the analysis considerably, will not have a major effect on the final result.

The vorticity in the wake can be expressed in terms of the unsteady component of the aerofoil circulation; the analysis of which is presented for a symmetrical aerofoil oscillating about a mean incidence of 0° (Fig.3). The wake vortex element shed from the trailing edge during any small time interval δt has a circulation equal and opposite to the corresponding change of aerofoil circulation, therefore just aft of the trailing edge the strength of the shed vorticity,

$$\gamma_W(x_T,t)\delta x = - \frac{\partial \Gamma}{\partial t} \delta t. \tag{15}$$

Assuming that the shed vorticity is moving with mean velocity U_∞, then

$$\delta x = U_\infty \delta t$$

thus

$$U_\infty \gamma_W(x_T,t) = - \frac{\partial \Gamma}{\partial t} \quad . \tag{16}$$

The vortex element at a general point x of the wake at time t was shed at an earlier time $(t - x/U_\infty)$, assuming that the wake vorticity is convected at the uniform velocity U_∞, thus

$$\gamma_W\left(x,\ t + \frac{[x-x_T]}{U_\infty}\right) = \gamma_W(x_T,\ t) \ . \tag{17}$$

Since all variables are assumed proportional to $e^{i\omega t}$, eqn. (16) becomes

$$U_\infty \gamma_{W_o}(x) e^{i\omega(t+[x-x_T]/U_\infty)} = - i\omega \Gamma_o e^{i\omega t} \quad , \tag{18}$$

where

$$\gamma_W(x,t) = \gamma_{W_o}(x) e^{i\omega t} \quad ,$$

so

$$\gamma_{w_0}(x) = -\frac{i\nu\Gamma_0}{c} e^{\{-i\nu(\bar{x}-\bar{x}_T)\}}. \tag{19}$$

The extension of the above analysis to the case of an aerofoil oscillating about a mean incidence is straightforward where $(x-x_T)$ is interpreted as the distance of a general point from the trailing edge measured along the appropriate mean streamline from the trailing edge. Again it is assumed that the vorticity is convected with constant velocity equal to U_∞.

2.3 KUTTA CONDITION

In order to find a unique value of the aerofoil circulation, Γ, a single Kutta condition at the trailing edge has to be applied. As discussed previously the Kutta condition for the present theory is taken to be equal pressure on the upper and lower surface at the trailing edge, that is the zero loading condition. It follows from the unsteady Bernoulli equation that

$$\{\tfrac{1}{2}[(\cos\alpha + \bar{u}_s + \bar{u}_0 e^{i\omega t})^2 + (\sin\alpha + \bar{w}_s + \bar{w}_0 e^{i\omega t})^2] + \frac{i\omega\phi_0 e^{i\omega t}}{U_\infty^2}\}_{\text{upper surface trailing edge}}$$

$$= \{[\tfrac{1}{2}(\cos\alpha + \bar{u}_s + \bar{u}_0 e^{i\omega t})^2 + (\sin\alpha + \bar{w}_s + \bar{w}_0 e^{i\omega t})^2] + \frac{i\omega\phi_0 e^{i\omega t}}{U_\infty^2}\}_{\text{lower surface trailing edge}}. \tag{20}$$

Equating terms independent of time gives the steady state condition

$$\{(\cos\alpha + \bar{u}_s)^2 + (\sin\alpha + \bar{w}_s)^2\}_{\text{upper surface trailing edge}} = \{(\cos\alpha + \bar{u}_s)^2 + (\sin\alpha + \bar{w}_s)^2\}_{\text{lower surface trailing edge}} \tag{21}$$

Equating terms in $e^{i\omega t}$ gives the fundamental boundary condition

$$\{(\cos\alpha + \bar{u}_s)\bar{u}_o + (\sin\alpha + \bar{w}_s)\bar{w}_o + i\nu\phi_o/U_\infty\}_{\text{upper surface trailing edge}}$$

$$= \{(\cos\alpha + \bar{u}_s)\bar{u}_o + (\sin\alpha + \bar{w}_s)\bar{w}_o + i\nu\phi_o/U_\infty\}_{\text{lower surface trailing edge}} . \tag{22}$$

Higher harmonics are neglected, as explained previously.

2.4 PRESSURE DISTRIBUTIONS, FORCES AND MOMENTS

The pressure relation in an incompressible time dependent fluid motion is derived from the unsteady Bernoulli equation, eqn. (6) which gives

$$c_p = \frac{p - p_\infty}{\frac{1}{2}\rho U_\infty^2} = 1 - \frac{q^2}{U_\infty^2} - \frac{2}{U_\infty^2}\frac{\partial\phi}{\partial t} , \tag{23}$$

where

$$\frac{q^2}{U_\infty^2} = (\cos\alpha + \bar{u}_s + \bar{u}_o e^{i\omega t})^2 + (\sin\alpha + \bar{w}_s + \bar{w}_o e^{i\omega t})^2 .$$

By definition

$$c_p = c_{p_s} + c_{p_o} e^{i\omega t} , \quad \phi = \phi_s + \phi_o e^{i\omega t} ,$$

hence, the unsteady pressure coefficient becomes

$$c_{p_o} = -2\,\bar{u}_o(\cos\alpha + \bar{u}_s) - 2\,\bar{w}_o(\sin\alpha + \bar{w}_s) - \frac{2i\nu\phi_o}{U_\infty c} . \tag{24}$$

The force and moment coefficients are obtained by direct integration of the pressure distribution given by eqn. (24).

3. TRANSLATIONAL OSCILLATION

The numerical method described for the pitching oscillation problem can be adapted for the translational (heaving) oscillation problem by modifying the surface boundary condition.

The simple harmonic translational motion of the aerofoil to be superimposed on the steady profile, given by eqn. (1), is denoted by,

$$h = h_o e^{i\omega t} \quad . \tag{25}$$

The point (X,Z) on the aerofoil at any time t defined in terms of fixed axes (Fig. 4), may be written as

$$\left.\begin{aligned} X &= x_s \quad , && \text{on upper and lower surface,} \\ Z &= \zeta_{s_u} + h_o e^{i\omega t} && \text{on upper surface ,} \\ &= \zeta_{s_\ell} + h_o e^{i\omega t} && \text{on lower surface .} \end{aligned}\right\} \tag{26}$$

From the eqns. (10) and (26), the boundary conditions for the translational motion become,

$$\sin\alpha + \bar{w}_s = (\cos\alpha + \bar{u}_s)\zeta'_{s_u}(x) \tag{27}$$

and

$$\bar{w}_o - \bar{u}_o\, \zeta'_{s_u}(\bar{x}) = i\,\frac{\omega c}{U_\infty}\frac{h_o}{c} = i\nu\,\bar{h}_o \quad . \tag{28}$$

Similar relations can be written down for the lower surface.

Eqn. (27) is the steady boundary condition while eqn. (28) may be considered as the incremental unsteady boundary condition relating $\bar{u}_o$ and $\bar{w}_o$.

4. SINUSOIDAL GUST RESPONSE

The problem of an aerofoil passing through a sinusoidal vertical gust can be treated by the present technique.

For a stationary wave of wavelength λ Fig. 5(a), the vertical gust velocity relative to aerofoil can be written as

$$w_g = w_{g_o} \sin\frac{2\pi}{\lambda}(x - U_\infty t) \tag{29}$$

or more conveniently this can be written

$$w_g = w_{g_o} e^{-i \frac{2\pi c}{\lambda} \bar{x}} e^{i \frac{2\pi U_\infty}{\lambda} t}$$

$$= w_{g_o} e^{-i\nu\bar{x}} e^{i\omega t} , \tag{30}$$

where

$$\omega = \frac{2\pi U_\infty}{\lambda}$$

and

$$\nu = \frac{\omega c}{U_\infty} , \tag{31}$$

For a travelling wave of velocity V as shown in Fig. 5(b), the vertical gust velocity relative to the aerofoil can be written in a similar manner

$$w_g = w_{g_o} e^{-i\left\{\frac{2\pi}{\lambda} \bar{x} - (U_\infty + V)t\right\}}$$

$$= w_{g_o} e^{-i\nu\bar{x}} e^{i\omega t} , \tag{32}$$

where

$$\omega = \frac{2\pi(U_\infty + V)}{\lambda}$$

and

$$\nu = \frac{\omega c}{U_\infty + V} . \tag{33}$$

Thus, a travelling gust may be thought of as a stationary gust having a modified frequency parameter. In the present investigation only results for the stationary gust have been derived.

The boundary condition in this case can be derived from eqn. (10) as follows:-

$$\left\{\frac{U_\infty \sin\alpha + w_s + w_o e^{i\omega t} + w_{g_o} e^{-i\nu\bar{x}} e^{i\omega t}}{U_\infty \cos\alpha + u_s + u_o e^{i\omega t}}\right\} = \zeta_{s_u}'(x) \text{ upper surface}, \quad = \zeta_{s_\ell}'(x) \text{ lower surface}. \tag{34}$$

Using the normalised velocity components the following relations are obtained for the upper surface

$$\sin\alpha + \bar{w}_s = \zeta_{s_u}'(\bar{x})(\cos\alpha + \bar{u}_s), \tag{35}$$

$$\bar{w}_o - \bar{u}_o \zeta_{s_u}'(\bar{x}) = -\bar{w}_{g_o} e^{-i\nu\bar{x}} . \tag{36}$$

Similar relations can be written for the lower surface. Again, eqn. (35) is the steady state boundary condition and eqn. (36) may be considered as the incremental unsteady boundary condition relating $\bar{u}_o$ and $\bar{w}_o$.

5. CONTROL SURFACE OSCILLATION

When a control surface oscillates about its hinge (Fig. 6) the unsteady boundary condition formulated in eqn. (10) is applied on the part of the surface defining the control surface. On the remaining stationary surface ahead of the oscillating control surface the modified boundary condition should then read,

$$\frac{U_\infty \sin\alpha + w_s + w_o e^{i\omega t}}{U_\infty \cos\alpha + u_s + u_o e^{i\omega t}} = \zeta_{s_u}'(x), \text{ on upper surface}, \quad = \zeta_{s_\ell}'(x), \text{ on lower surface}. \tag{37}$$

Using a normalised velocity the following relations are obtained for the upper surface; on the stationary aerofoil ahead of the control surface

$$\bar{w}_o - \bar{u}_o \zeta_{s_u}'(\bar{x}) = 0 , \tag{38}$$

and on the oscillating control surface

$$\bar{w}_o - \bar{u}_o \bar{\zeta}_{s_u}'(\bar{x}) = -\delta_o\{(\cos\alpha + \bar{u}_s) + (\sin\alpha + \bar{w}_s)\bar{\zeta}_{s_u}'(\bar{x}) + i\nu(\bar{x}_s + \bar{\zeta}_{s_u}(\bar{x})\bar{\zeta}_{s_u}'(\bar{x})\}. \tag{39}$$

Similar relations can be written down for the lower surface.

6. METHOD OF SOLUTION

The potential flow problem formulated above is solved by superimposing the fields of a distribution of sources and vorticity situated on the mean aerofoil surface in a uniform stream. The strengths of the distributions are adjusted in such a way that the resulting velocity field satisfies the prescribed boundary conditions and the trailing edge Kutta condition. The numerical procedure is similar to the one used in solving the steady problem[10].

The continuous steady (mean) aerofoil surface is approximated by N straight elements as shown in Fig. (7). The numbering of the elements starts at the trailing edge on the lower surface and proceeds around the aerofoil surface in the clockwise sense.

A uniform source distribution of strength $(\sigma_{s_i} + \sigma_{o_i} e^{i\omega t})$ is placed on the i^{th} element together with a uniform vorticity distribution $(\gamma_s + \gamma_o e^{i\omega t})$. The strengths σ_{s_i}, σ_{o_i} vary from element to element but γ_s, γ_o are taken to be the same for all elements on the aerofoil profile. It is to be noted that σ_{o_i} and γ_o are complex with inphase and out-of-phase components.

Because the wake extends to infinity downstream the vorticity in the wake cannot be represented by a finite number of elements. It is assumed here that only the first chord length of the wake behind the trailing edge need be represented by finite elements. The effect of the remainder of the wake is calculated analytically by making the assumption that only downwash is induced at the aerofoil by this far wake. For one chord behind the aerofoil a number (M) of straight line elements are taken similar to those on aerofoil profile and the uniform vortex strength of each of these wake elements is taken to be the vorticity strength at the centre of each element, as given by eqn. (19), thus

$$\left(\gamma_{w_o}\right)_k = -\frac{i\nu\Gamma_o}{c}\exp\{-i\nu(\bar{x}_k - \bar{x}_T)\} \ . \tag{40}$$

Defining $\bar{\sigma}_{s_i}$, $\bar{\sigma}_{o_i}(=\frac{\sigma}{U_\infty c})$, and $\bar{\gamma}_s$, $\bar{\gamma}_o(=\frac{\gamma}{U_\infty})$ normalised with respect to c and U_∞, the normalised perturbation velocities due to the distribution of sources and vorticity can be expressed in the form

$$\left.\begin{aligned} \bar{u}_{s_j} &= \sum_{i=1}^{N} A_{ji}\,\bar{\sigma}_{s_i} + \bar{\gamma}_s \sum_{i=1}^{N} B_{ji} \ , \quad \bar{u}_{o_j} = \sum_{i=1}^{N} A_{ji}\,\bar{\sigma}_{o_i} + \bar{\gamma}_o \sum_{i=1}^{N} B_{ji} \\ \bar{w}_{s_j} &= \sum_{i=1}^{N} B_{ji}\,\bar{\sigma}_{s_i} - \bar{\gamma}_s \sum_{i=1}^{N} A_{ji} \ , \quad \bar{w}_{o_j} = \sum_{i=1}^{N} B_{ji}\,\bar{\sigma}_{o_i} - \bar{\gamma}_o \sum_{i=1}^{N} A_{ji} \end{aligned}\right\} \ , \tag{41}$$

where $\bar{u}_{s_j}$, $\bar{u}_{o_j}$, $\bar{w}_{s_j}$, $\bar{w}_{o_j}$ are the perturbation velocities at the centre point of the j^{th} element induced by the distribution of unit sources and vorticity on the aerofoil and A_{ji}, B_{ji} are the appropriate influence coefficients as derived in Appendix I. These coefficients A_{ji}, B_{ji} depend only on the co-ordinates of the i^{th} and j^{th} elements.

The contribution to the velocity components due to the first chord length of the wake behind the trailing edge can be expressed in the form

$$\begin{aligned} \bar{u}_{o_j} &= \sum_{k=1}^{M} B_{jk}\left(\gamma_{w_o}\right)_k = -i\nu\bar{\gamma}_o\,(\Delta/c)\sum_{k=1}^{M} B_{jk}\,e^{-i\nu(\bar{x}_k - \bar{x}_T)} \ , \\ \bar{w}_{o_j} &= -\sum_{k=1}^{M} A_{jk}\left(\gamma_{w_o}\right)_k = i\nu\bar{\gamma}_o\,(\Delta/c)\sum_{k=1}^{M} A_{jk}\,e^{-i\nu(\bar{x}_k - \bar{x}_T)} \ , \end{aligned} \tag{42}$$

where Δ is the total aerofoil perimeter ($= \sum_{i=1}^{N}$ (elemental lengths)) $= \sum_{i=1}^{N}\Delta_i$) and where the influence coefficients A_{ij} and B_{ij} are the same as those in eqns. (41).

The remainder of the wake aft of one chord behind the trailing edge is retained as a continuous distribution of vorticity and it is assumed to lie in the free stream direction; furthermore it is assumed that the velocity field due to this far wake is a downwash field only. This assumption is valid for a symmetrical aerofoil oscillating about zero degree incidence and it is believed that this assumption is

reasonable for a general aerofoil oscillating about a small mean angle of incidence. The downwash field due to this far wake is derived in Appendix II and is given as

$$\bar{w}_{o_j} = i\nu \frac{\bar{\gamma}_o}{2\pi} \frac{\Delta}{c} e^{-i\nu(\bar{x}_j - \bar{x}_T)} \{C_i[\nu(1 - (\bar{x}_j - \bar{x}_T))] - i(S_i[\nu(1 - (\bar{x}_j - \bar{x}_T))] - \frac{\pi}{2})\} \quad , \tag{43}$$

where

$$C_i(\xi) = - \int_{\xi}^{\infty} \frac{\cos\lambda}{\lambda} d\lambda$$

$$S_i(\xi) = - \int_{\xi}^{\infty} \frac{\sin\lambda}{\lambda} d\lambda + \frac{\pi}{2} \quad ,$$

are standard tabulated functions.

The steady state solution for $\bar{u}_s$, $\bar{w}_s$, c_{p_s} is obtained by satisfying the steady state boundary condition, eqn. (12), along with the Kutta condition, eqn. (21), as applied in the steady state. The procedure, which is standard, is outlined in more detail in reference 10.

The unsteady problem is solved by satisfying the appropriate unsteady boundary condition, eqns. (13)(or (28) or (36) or (38),(39)), along with the Kutta condition, Eqn. (22). In setting up the Kutta condition the value of the difference in unsteady component of the perturbation velocity potential, ϕ_o, is required at the trailing edge. This difference is the circulation Γ_o around the aerofoil and the Kutta condition eqn. (22) can be written in terms of $\Gamma_o (= \Delta \gamma_o)$ instead of ϕ_o. Thus (N+1) linear simultaneous equations can be set up using eqns. (13), (22), (41), (42) and (43). These simultaneous complex equations are solved for $\bar{\sigma}_{o_i}$ and $\bar{\gamma}_o$ by a successive orthogonalization technique.

Once the source and vorticity strengths have been determined then the velocity distribution on the aerofoil surface is known from eqns. (43). However for the calculation of the unsteady pressure coefficient, c_{p_o}, the velocity potential ϕ_o is also required over the surface.

The velocity potential due to the source distribution is simple and straightforward and can be easily written down in terms of the source strengths. The perturbation potential at the mid point of the j^{th} element due to the source distribution σ_{o_j} can be written as

$$\phi_{o_j} = \sum_{i=1}^{N} \frac{\sigma_{o_i}}{2\pi} \left\{ \frac{(\Delta_i/2 - x_{ji})}{2} \ell n[(\Delta_i/2 - x_{ji})^2 + z_{ji}^2] \right.$$

$$+ \frac{(\Delta_i/2 + x_{ji})}{2} \ell n[(\Delta_i/2 + x_{ji})^2 + z_{ji}^2] - \Delta_i$$

$$\left. + z_{ji}[\tan^{-1}(\frac{\Delta_i/2 - x_{ji}}{z_{ji}}) + \tan^{-1}(\frac{\Delta_i/2 + x_{ji}}{z_{ji}})] \right\} . \qquad (44)$$

The mathematical derivation is given in Appendix III, together with the notation.

The perturbation potential due to the vorticity distribution presents some difficulty. An expression similar to that due to the source distribution given by eqn. (44) cannot easily be derived. The difficulty is associated with the cut necessary to ensure that ϕ is single valued. In this case the cut has to be taken to coincide with the aerofoil surface and the wake. A complete analysis of this procedure is given by Giesing[5]. The procedure is complicated and in the present method a simplified approach is adopted.

Since

$$d\phi = udx + wdz$$

and since the velocities (u,w) are already computed in terms of σ, γ and influence coefficients, then ϕ can be calculated by integrating the velocities around the surface from the nose of the aerofoil. Thus, the perturbation potential at the j^{th} mid point due to the circulatory flow field is given by

$$\phi_j = \sum_{i=\frac{N}{2}+1}^{j-1} \{u_{o_i}' \Delta_i \cos\theta_i + w_{o_i}' \Delta_i \sin\theta_i\} + u_{o_j}' \frac{\Delta_j}{2} \cos\theta_j + w_{o_j}' \frac{\Delta_j}{2} \sin\theta_j \tag{45}$$

on the upper surface, and

$$\phi_j = \sum_{i=j-1}^{N/2} \{u_{o_i}' \Delta_i \cos\theta_i + w_{o_i}' \Delta_i \sin\theta_i\} + u_{o_j}' \frac{\Delta_j}{2} \cos\theta_j + w_{o_j}' \frac{\Delta_j}{2} \sin\theta_j$$

on the lower surface, where u_{o_i}' and w_{o_i}' are the velocity components due to the vorticity distribution only. The perturbation velocity potential of the entire flow field is the sum of eqns. (44) and (45) plus a possible arbitrary constant. This constant, which is only required for the pressures but not for the evaluation of force and moment coefficients, is zero for a symmetrical aerofoil oscillating about zero incidence. For aerofoils with mean incidence and/or camber this constant can be evaluated by integrating the upstream velocity field due to the circulatory flow along a suitable line up to the leading edge, the constant is found to be very small for all the aerofoils considered in this paper.

The overall force and moment coefficients are obtained by numerical integration:

$$C_x = \left(\sum_{i=1}^{N} c_{p_{o_i}} \bar{\Delta}_i \sin\theta_i\right) e^{i\omega t} \quad ,$$

$$C_z = \left(\sum_{i=1}^{N} c_{p_{o_i}} \bar{\Delta}_i \cos\theta_i\right) e^{i\omega t} \quad ,$$

$$C_{M_o} = \left(\sum_{i=1}^{N} c_{p_{o_i}} \bar{\Delta}_i [- x_i \cos\theta_i - z_i \sin\theta_i]\right) e^{i\omega t} \quad .$$

A programme has been developed in FORTRAN IV which solves the sets of simultaneous real and complex equations directly by the successive orthogonalization method. The programme in its present form requires a core size of 87 K on the I.C.L. 1904 S, including system and programme, for up to 180 elements on the aerofoil surface and 30 elements on the wake. The computer time increases rapidly with the increase of number of aerofoil elements. The determination of optimum number of elements for a specified accuracy for oscillating aerofoil problems has not been completely pursued. The number of elements chosen for the numerical solutions presented in this paper is based on the experience gained for steady aerofoil problems.

For a clean steady aerofoil (without deflected control surfaces) it has been found that a relatively small number of elements (about 50) gives adequate accuracy. However, for an aerofoil fitted with a control surface it is found that a large number of elements is needed particularly on the control surface. It has been observed that increased accuracy beyond a certain number of elements is not very significant. For example, it has been found that for an aerofoil with 30% control surface chord 130 elements (50 on the aerofoil + 80 on control surface) give steady hinge moment coefficients within 3% of results obtained using 250 elements (120 + 130). Similar trends have been observed for limited numerical studies of the oscillating aerofoil problems.

In the presented results a small number of elements (usually about 50) have been used for aerofoils without any control surfaces (Figs. 11 - 21), and 132 elements have been used for oscillating control surfaces (Figs. 21 - 24).

7. RESULTS AND DISCUSSIONS

To check its accuracy the present method has been applied to the aerofoil shape studied by Van de Vooren and Van de Vel[7]. The aerofoil shape, given in reference 7, is repeated here for convenience,

$$x - \frac{c}{2} + iz = \frac{(ae^{i\theta} - a)^{1.9}}{(ae^{i\theta} - 0.05a)^{0.09}} \; ; \quad \frac{a}{c} = \frac{1}{2}\left(\frac{1.05}{2}\right)^{0.9}.$$

The aerofoil is symmetrical with a trailing edge angle 18°. The maximum thickness of this profile is about 14.4% and lies at a distance of 30.8% of the chord behind the leading edge. The unsteady pressure distribution has been evaluated for the aerofoil oscillating in simple harmonic motion about the mid chord position. The frequency parameter of the oscillation is 0.8 and the mean angle of incidence is zero.

A comparison of the numerical results derived by the present method with the analytic solution is shown in Fig. 10. The comparison shows clearly that the unsteady pressure distribution both in-phase and out-of-phase agree well with the analytic solution. There appears to be a small difference in the pressure coefficient between the present method and the analytic solution for a few points near the leading edge. This difference may be due to the inaccurate plotting of the analytic solution which has been reproduced by reading off the points from Fig. 2 of reference 7. It is also possible that the number of elements considered near the leading edge of the aerofoil is not sufficient for the desired accuracy.

Linearised theory result has been plotted in Fig. 10 to show the difference between linearised and non-linear theory. It can be seen that linearised theory underestimates the pressure in certain regions and overestimates in other regions.

Figs. 11, 12(a) and 12(b) give the oscillating pressure distributions as calculated by the present numerical method for frequency

parameters of 0, 0.5, and 1.0, for the de Vooren and de Vel aerofoil at two mean incidences. Fig. 11 gives the pressure distribution for a mean angle of incidence of 0°. Figs. 12(a) and 12(b) give the pressure distribution when mean angle of incidence is 10°; in Fig. 12(b) the scale of c_p has been reduced to show the behaviour of the pressure near the peak suction. These graphs indicate that the pressure distribution for different frequency parameters is similar in nature. They also show that the in-phase pressure distribution has a converging tendency with increasing frequency parameter, this tendency is confirmed later when overall lift and moment coefficients are shown.

The present method has been applied to two Karman-Trefftz aerofoil sections, one symmetric, the other cambered with 8.6% camber, oscillating about the mid chord position at the mean angles of incidence of 0° and 10°. Both of these aerofoils have the same trailing edge angle of 10° and thickness/chord ratio approximately 13%. The lift and moment coefficients of these aerofoils at the mean angles of incidence of 0° and 10° are plotted in Figs. 13 and 14. The moment coefficient C_M is taken about the axis of rotation which is situated at the half chord position. The effect of mean angle of incidence on lift and moment coefficients is seen to be significant for the cambered aerofoil. Linearised theory results are also plotted in the same diagrams to illustrate the non-linear effects; there are differences especially in the in-phase components of both C_L and C_M at lower frequency parameters. To see the effects of camber more clearly the lift and moment coefficients of these two aerofoils at the same mean angle of incidence are plotted in Figs. 15(a) and 15(b). Again it can be seen from these graphs that the combination of mean incidence and camber can lead to a significant difference in the in-phase components of C_L and C_M.

The results of the 8.4% thick symmetrical Von Mises aerofoil performing a simple harmonic heaving oscillation at 0° incidence are plotted in Figs. 16 and 17. Fig. 16 gives the pressure distribution at different frequency parameters and Fig. 17 gives the overall lift and moment coefficients along with the linearised theory results. The thickness effect is usually small for small values of frequency parameter but for large values of frequency parameter the thickness effect changes the values of lift and moment coefficients by about 5 - 10%.

The results of the 8.4% thick symmetrical Von Mises aerofoil passing through a sinusoidal (vertical) gust are plotted in Figs. 18 and 19. Fig. 18 shows the pressure difference at various frequency parameters. Fig. 19 shows the overall lift and moment coefficients along with the linearised theory results. It is seen that for smaller values of frequency parameter (up to about $\nu = 1$) the difference between the linearised solution and the solution of the present method is small, however beyond the value of $\nu = 1$ the difference is still small for the out-of-phase components of the lift and moment coefficients, but the difference seems to increase progressively with ν for the in-phase component of these coefficients. The difference in the in-phase component of the lift is about 20% when $\nu = 2$. The percentage difference in the pitching moment about the quarter chord point is perhaps not a fair comparison because the linearised pitching moment is zero for all values of ν. A better comparison would be to consider the shift of the centre of pressure. According to linearised theory the lift always acts at the quarter chord point while the present theory shows a forward shift of the in phase aerodynamic centre with the frequency parameter. The shift is of the order of 8% of the chord for the range of frequency parameter considered.

The present technique has been applied to the case of an oscillating control surface on a symmetrical and a cambered (8.6%) Karman-Trefftz aerofoil. The control surface chord is taken to be 30% of the aerofoil chord. The results have been plotted in Figs. 20, 21, 22 and 23. Fig. 20 gives the pressure distribution at various frequency parameters. Fig. 21(a) shows the overall lift and moment (about the quarter chord) coefficients while Fig. 21(b) shows the hinge moment coefficients for a symmetrical Karman-Trefftz aerofoil, it is seen that the in phase hinge moment is significantly affected by thickness as indicated by the difference with linearised theory. Figs. 22(a) and 22(b) give the similar results for the cambered aerofoil. Fig. 23 gives the results for symmetrical Karman-Trefftz aerofoil at mean angle of incidence of 0° when the control surface oscillates about a mean control surface angle of 5°.

Mean aerofoil incidence has a little effect for both symmetrical and cambered aerofoils. It is noticed that camber has some effect on the overall lift, pitching moment and hinge moment coefficients for both in- and out-of-phase components; this effect is especially large (about 18%) for the in-phase component of the hinge moment coefficient. Mean control surface angle does not introduce any measurable changes.

As deduced from the comparison of linearised and non-linear theory thickness effect on the overall lift due to control surface oscillation is small for a symmetrical aerofoil but more noticeable for a cambered aerofoil. Thickness effect on the moment coefficients for both symmetrical and cambered aerofoils are significant.

The thickness effect on the out-of-phase components of the hinge moment coefficient is small for both symmetrical and cambered aerofoils, but thickness effects are especially large for the in-phase component of

the hinge moments; the in-phase component of C_H is approximately 80% of the linearised value for symmetrical aerofoil and 67% of the linearised value for the cambered aerofoil.

8. CONCLUDING REMARKS

(a) A method has been developed for the calculation of the pressure distribution on an oscillating aerofoil in incompressible flow conditions by the extension of the A.M.O. Smith technique. Singularity distributions are placed on the steady mean aerofoil profile; the oscillatory boundary conditions are satisfied on this mean profile.

(b) It is argued that the appropriate Kutta condition in the present approach is the condition of zero loading at the trailing edge.

(c) Satisfactory agreement has been obtained between the present numerical approach and an analytic solution for a pitching aerofoil (see Fig. 11).

(d) For a pitching aerofoil there is noticeable difference in the pressure distribution between the present method and linearised theory (see Fig. 11). Although linearised theory gives the correct trends for C_L and C_M for an aerofoil in oscillatory conditions the linearised values of C_L and C_M can be in error by the order of 10% (see Figs. 14, 18, 20).

(e) The combined effects of mean angle of incidence and the camber of a pitching aerofoil can affect C_L and C_M (see Fig. 16).

(f) Similar trends occur for a heaving aerofoil and aerofoil passing through a sinusoidal gust.

(g) For an oscillating control surface the most significant result is that the in-phase component of the hinge moment coefficient is considerably less than the values predicted by linearised theory (Figs. 22, 23).

REFERENCES

1. Hess, J.L. and Smith, A.M.O. Calculation of Potential Flow about Arbitrary Bodies. Progress in Aeronautical Sciences, Vol. 8.

2. Hess, J.L. Calculation of Potential Flow about Bodies of Revolution having Axes Perpendicular to the Free Stream Direction. D.A.C. Report No. 29812, 1960.

3. Hess, J.L. Calculation of Potential Flow about Arbitrary Three Dimensional Lifting Bodies. Douglas A/C Report, No. MDC J5679-01, 1972.

4. Giesing, J.P. Non-linear Two Dimensional Potential Flow with Lift. Journal of Aircraft Vol. 5, No. 2, March-April 1968.

5. Giesing, J.P. Two Dimensional Potential Flow Theory for Multiple Bodies in Small Amplitude Motion. D.A.C. Report No. 67028, 1968.

6. Kussner, H.G. and Gorup, G.V. Instationare linearisierte Theorie der Flugelprofile endlicher Dicke in Inkompressibles Stromung Mitt. des Max. Planch - Instituts fur Stromung - strorschung U. der Aerodynamischen Versrichsenstalt, Nr 26, Gottingen, 1960.

7. Van de Vooren, A.I. and Van de Vel, H. Unsteady Profile Theory in Incompressible Flow. Archiwurn Mechaniki Strosowanej 3, Vol. 16, 1964.

8. Hewson-Brown, R.C. The Oscillation of a Thick Aerofoil in an Incompressible Flow. Mechanics and Applied Mathematics, Vol. XVI, Feb. 1963.

9. Basu, B.C. and Hancock, G.J. The Unsteady Motion of a Two Dimensional Aerofoil in Incompressible Inviscid Flow. QMC - EP 1018, 1976.

10. Hancock, G. J. and Padfield, G. Numerical Solution for Two-Dimensional Aerofoil in Incompressible Flow. QMC - EP 1003, 1972.

APPENDIX I

The Influence Coefficients

A source distribution between $-\frac{\Delta}{2} < \bar{x} < \frac{\bar{\Delta}}{2}$ (as shown in Fig. 8(a)) with normalised strength $\bar{\sigma}$/unit length is considered.

The velocity components $\delta\bar{u}$ and $\delta\bar{w}$ at the point (x, z) due to the small element of source distribution on $\delta\xi$ are

$$\left.\begin{aligned} \delta\bar{u}(\bar{x},\bar{z}) &= \frac{\bar{\sigma}}{2\pi}\left[\frac{\bar{x}-\bar{\xi}}{(\bar{x}-\bar{\xi})^2+\bar{z}^2}\right]\delta\bar{\xi} \\ \delta\bar{w}(\bar{x},\bar{z}) &= \frac{\bar{\sigma}}{2\pi}\left[\frac{\bar{z}}{(\bar{x}-\bar{\xi})^2+\bar{z}^2}\right]\delta\bar{\xi} \end{aligned}\right\} . \qquad (A.1)$$

On integration

$$\begin{aligned} \bar{u}(\bar{x},\bar{z}) &= \frac{\bar{\sigma}}{2\pi}\int_{-\bar{\Delta}/2}^{\bar{\Delta}/2}\left[\frac{\bar{x}-\bar{\xi}}{(\bar{x}-\bar{\xi})^2+\bar{z}^2}\right]d\bar{\xi} \\ &= \frac{\bar{\sigma}}{4\pi}\,\ell n\left[\frac{(\bar{x}+\bar{\Delta}/2)^2+\bar{z}^2}{(\bar{x}-\bar{\Delta}/2)^2+\bar{z}^2}\right] = \bar{\sigma}F(\bar{x},\bar{z},\bar{\Delta}), \end{aligned} \qquad (A.2)$$

$$\begin{aligned} \bar{w}(\bar{x},\bar{z}) &= \frac{\bar{\sigma}}{2\pi}\int_{-\bar{\Delta}/2}^{\bar{\Delta}/2}\frac{\bar{z}}{(\bar{x}-\bar{\xi})^2+\bar{z}^2}\,d\bar{\xi} \\ &= \frac{\bar{\sigma}}{2\pi}\,\tan^{-1}\left(\frac{\bar{x}+\bar{\Delta}/2}{\bar{z}}\right) - \tan^{-1}\left(\frac{\bar{x}-\bar{\Delta}/2}{\bar{z}}\right) = \bar{\sigma}G(\bar{x},\bar{z},\bar{\Delta}). \end{aligned} \qquad (A.3)$$

In equation (A.3)

$$-\frac{\pi}{2} < \tan^{-1}\theta \leq \frac{\pi}{2}$$

this condition gives the correct velocity distribution, i.e. antisymmetric $\bar{w}$ and symmetric $\bar{u}$, about the $\bar{x}$ axis.

As $\bar{x} \to 0$, $\bar{z} \to +0$ then

$$u(0,+0) \to 0$$

$$w(0,+0) \to \frac{\sigma}{2} \ ,$$

while for $\bar{x} \to 0$, $\bar{z} \to -0$

$$u(0,-0) \to 0$$

$$w(0,-0) \to -\frac{\sigma}{2} \ . \qquad \text{(A.4)}$$

Since elements are at different orientation the problem is transformed to a fixed axis system $(\bar{X},\bar{Z})$ as shown in Fig. 8(b); the origin of the $(\bar{X},\bar{Z})$ system is taken at the wing leading edge.

For the source distribution along a particular aerofoil element the normalised velocity components $\bar{u}(\bar{X},\bar{Z})$ and $\bar{w}(\bar{X},\bar{Z})$ axes,

$$\left.\begin{aligned} \bar{u}(\bar{X},\bar{Z}) &= \bar{\sigma}\{F(\bar{x},\bar{z},\bar{\Delta})\cos\theta - G(\bar{x},\bar{z},\bar{\Delta})\sin\theta\} \\ \bar{w}(\bar{X},\bar{Z}) &= \bar{\sigma}\{F(\bar{x},\bar{z},\bar{\Delta})\sin\theta + G(\bar{x},\bar{z},\bar{\Delta})\cos\theta\} \ , \end{aligned}\right\} \qquad \text{(A.5)}$$

where

$$\left.\begin{aligned} \bar{x} &= (\bar{X} - \bar{X}_0)\cos\theta + (\bar{Z} - \bar{Z}_0)\sin\theta \\ \bar{z} &= -(\bar{X} - \bar{X}_0)\sin\theta + (\bar{Z} - \bar{Z}_0)\cos\theta \ . \end{aligned}\right\} \qquad \text{(A.6)}$$

The influence of element i on the mid point of element j as shown in Fig. 8(c) is therefore written in the form

$$\begin{aligned} \bar{u}_{ji} &= \{F_{ji}\cos\theta_i - G_{ji}\sin\theta_i\}\,\bar{\sigma}_i \\ &= A_{ji}\,\bar{\sigma}_i \quad \text{for } i \neq j \ , \end{aligned} \qquad \text{(A.7)}$$

$$\begin{aligned} \bar{w}_{ji} &= \{F_{ji}\sin\theta_i + G_{ji}\cos\theta_i\}\,\bar{\sigma}_i \\ &= B_{ji}\,\bar{\sigma}_i \quad \text{for } i \neq j \ , \end{aligned} \qquad \text{(A.8)}$$

where

$$F_{ji} = F(\bar{x}_{ji},\bar{z}_{ji},\bar{\Delta}_i), \quad G_{ji} = G(\bar{x}_{ji},\bar{z}_{ji},\bar{\Delta}_i), \qquad \text{(A.9)}$$

and where

$$\left.\begin{aligned}
\bar{x}_{ji} &= \tfrac{1}{2}\{([\bar{X}_{j+1}+\bar{X}_j] - [\bar{X}_{i+1}+\bar{X}_j])\cos\theta_i + ([\bar{Z}_{j+1}+\bar{Z}_j] - [\bar{Z}_{i+1}+\bar{Z}_i])\sin\theta_i\} \\
\bar{z}_{ji} &= \tfrac{1}{2}\{-([\bar{X}_{j+1}+\bar{X}_j] - [\bar{X}_{i+1}+\bar{X}_i])\sin\theta_i + ([\bar{Z}_{j+1}+\bar{Z}_j] - [\bar{Z}_{i+1}+\bar{Z}_i])\cos\theta_i\} \\
\bar{\Delta}_i &= \{(\bar{X}_{i+1}-\bar{X}_i)^2 + (\bar{Z}_{i+1}-\bar{Z}_i)^2\}^{\frac{1}{2}} \\
\cos\theta_i &= \frac{\bar{X}_{i+1}-\bar{X}_i}{\bar{\Delta}_i} \quad , \quad \sin\theta_i = \frac{\bar{Z}_{i+1}-\bar{Z}_i}{\bar{\Delta}_i} \quad .
\end{aligned}\right\} \qquad (A.10)$$

In the limiting case

$$\left.\begin{aligned}
\bar{u}_{ii} &= \left\{-\frac{\sin\theta_i}{2}\right\}\bar{\sigma}_i = A_{ii}\,\bar{\sigma}_i \quad , \\
\bar{w}_{ii} &= \left\{\frac{\cos\theta_i}{2}\right\}\bar{\sigma}_i = B_{ii}\,\bar{\sigma}_i \quad .
\end{aligned}\right\} \qquad (A.11)$$

For a normalised vortex distribution γ on an element as shown in Fig. 9 the velocity components $\delta\bar{u}$ and $\delta\bar{w}$ at point $(\bar{x},\bar{z})$ due to circulation around $\delta\bar{\xi}$

$$\left.\begin{aligned}
\delta\bar{u} &= \frac{\bar{\gamma}}{2\pi}\left[\frac{\bar{z}}{(\bar{x}-\bar{\xi})^2 + \bar{z}^2}\right]\delta\bar{\xi} \\
\delta\bar{w} &= -\frac{\bar{\gamma}}{2\pi}\left[\frac{\bar{x}-\bar{\xi}}{(\bar{x}-\bar{\xi})^2 + \bar{z}^2}\right]\delta\bar{\xi}
\end{aligned}\right\} . \qquad (A.12)$$

It is seen that equations (A.12) for $\bar{u}$ and $\bar{w}$ due to $\bar{\gamma}$ are the same as $\delta\bar{w}$ and $-\delta\bar{u}$ due to $\bar{\sigma}$ in equations (A.1). Thus without further ado the velocities induced by the elements of vorticity may be written

$$\left.\begin{aligned}
\bar{u}_{ji} &= B_{ji}\bar{\gamma} \\
\bar{w}_{ji} &= -A_{ji}\bar{\gamma} \quad .
\end{aligned}\right\} \qquad (A.13)$$

APPENDIX II

The Downwash Field due to the Semi-infinite Wake

The part of the wake beyond one chord length from the trailing edge of the aerofoil is assumed to be in a plane parallel to the free stream direction. The downwash field along the chord line due to this far wake is assumed to be the same as that due to a wake in the chordal plane extending from $(1+\bar{x}_T)$ to ∞.

The downwash at any point $\bar{x}$ on the chordline due to this wake is given by

$$\bar{w}(\bar{x},t) = -\frac{1}{2\pi}\int_{1+\bar{x}_T}^{\infty} \frac{\bar{\gamma}_w(\bar{\xi},t)d\bar{\xi}}{\bar{\xi}-\bar{x}} \quad . \tag{A.14}$$

Now

$$\bar{w}(\bar{x},t) = \bar{w}_o(\bar{x})e^{i\omega t} \text{ and } \bar{\gamma}_w(\bar{x},t) = \bar{\gamma}_{w_o}(\bar{x})e^{i\omega t} \quad .$$

Therefore,

$$\bar{w}_o(\bar{x}) = \frac{1}{2\pi}\int_{1+\bar{x}_T}^{\infty} \frac{\bar{\gamma}_{w_o}(\bar{\xi})d\bar{\xi}}{\bar{\xi}-\bar{x}} \quad . \tag{A.15}$$

Using eqn. (19),

$$\bar{w}_o(\bar{x}) = -\frac{i\nu}{2\pi} e^{-i\nu(\bar{x}-\bar{x}_T)} \gamma_o\left(\sum_{i=1}^{N} \frac{\bar{\Delta}_i}{c}\right) \int_{\nu[1-(\bar{x}-\bar{x}_T)]}^{\infty} \frac{e^{-i\lambda}}{\lambda} d\lambda \quad . \tag{A.16}$$

Thus

$$\bar{w}_o(\bar{x}) = \frac{i\nu}{2\pi} \bar{\gamma}_o\left(\sum_{i=1}^{N} \bar{\Delta}_i\right)e^{i\nu(\bar{x}-\bar{x}_T)}[\{C_i[1-(\bar{x}-\bar{x}_T)]\nu - i\{S_i[1-(\bar{x}-\bar{x}_T)]\nu - \frac{\pi}{2}\}] \tag{A.17}$$

where

$$C_i(\xi) = -\int_{\xi}^{\infty} \frac{\cos\lambda}{\lambda}\, d\lambda$$

$$S_i(\xi) = -\int_{\xi}^{\infty} \frac{\sin\lambda}{\lambda}\, d\lambda + \frac{\pi}{2}$$

are the standard functions.

APPENDIX III

The Perturbation Potential due to the Unsteady Flow Field

The perturbation potential of the unsteady flow field is that due to the source and vortex distribution.

The potential due to a source distribution with normalised strength $\bar{\sigma}$/unit length along x-axis (Fig. 8(a)) between the limit $-\frac{\bar{\Delta}}{2} < \bar{x} < \frac{\bar{\Delta}}{2}$ is

$$\int_{-\bar{\Delta}/2}^{\bar{\Delta}/2} \frac{\bar{\sigma}}{4} \ell n\{(\bar{x} - \bar{\xi})^2 + \bar{z}^2\}\, d\bar{\xi} \quad . \tag{A.19}$$

If $\bar{\sigma}$ is constant the potential becomes

$$\frac{\bar{\sigma}}{2\pi}\left[\frac{(\bar{\Delta}/2 - \bar{x})}{2} \ell n\{(\bar{\Delta}/2 - \bar{x})^2 + \bar{z}^2\} + \frac{(\bar{\Delta}/2 + \bar{x})}{2} \ell n\{(\bar{\Delta}/2 + \bar{x})^2 + \bar{z}^2\} - \bar{\Delta}\right.$$
$$\left. + \bar{z}\{\tan^{-1}\left(\frac{\bar{\Delta}/2 - \bar{x}}{2}\right) + \tan^{-1}\left(\frac{\bar{\Delta}/2 + \bar{x}}{2}\right)\}\right] . \tag{A.20}$$

The potential at the mid point of the j^{th} element due to the source on the i^{th} element, using the notation of eqns. (A.10), is

$$\frac{\bar{\sigma}_i}{2}\left[\frac{(\bar{\Delta}_i/2 - \bar{x}_{ji})}{2} \ell n\,(\bar{\Delta}_i/2 - \bar{x}_{ji})^2 + \bar{z}_{ji}^{\,2}\} + \frac{(\bar{\Delta}_i/2 + \bar{x}_{ji})}{2} \ell n\,(\bar{\Delta}_i/2 + \bar{x}_{ji})^2 + \bar{z}_{ji}^{\,2}\}\right.$$
$$\left. - \bar{\Delta}_i + \bar{z}_{ji}\{\tan^{-1}\frac{(\bar{\Delta}_i/2 - \bar{x}_{ji})}{\bar{z}_{ji}} + \tan^{-1}\frac{(\bar{\Delta}_i/2 + \bar{x}_{ji})}{\bar{z}_{ji}}\}\right] . \tag{A.21}$$

The total potential at the j^{th} mid point due to the entire source distribution is therefore

$$\phi_{o_j} = \sum_{i=1}^{N}\left[\frac{\bar{\sigma}_i}{2}\frac{(\bar{\Delta}_i/2 - \bar{x}_{ji})}{2} \ell n\{(\bar{\Delta}_i/2 - \bar{x}_{ji}) + \bar{z}_{ji}^{\,2}\}\right.$$
$$+ \frac{(\bar{\Delta}_i/2 + \bar{x}_{ji})}{2} \ell n\{(\bar{\Delta}_i/2 + \bar{x}_{ji})^2 + \bar{z}_{ji}^{\,2}\} - \bar{\Delta}_i \tag{A.22}$$
$$\left. + \bar{z}_{ji}\{\tan^{-1}\left(\frac{\bar{\Delta}_i/2 - \bar{x}_{ji}}{\bar{z}_{ji}}\right) + \tan^{-1}\left(\frac{\bar{\Delta}_i/2 + \bar{x}_{ji}}{\bar{z}_{ji}}\right)\}\right] \quad .$$

The perturbation potential due to the vorticity distribution

$$\phi_o = \int_o^x u_o' \, dx + \int_o^z w_o' \, dz \tag{A.23}$$

where u_o' and w_o' are the perturbation potential velocity components due to the circulatory flow only.

Thus the potential at the j^{th} mid point due to the circulatory flow field:

on upper surface

$$\phi_{o_j} = \sum_{i=\frac{N}{2}+1}^{j-1} (u_{o_i}' \bar{\Delta}_i \cos\theta_i + w_{o_i}' \bar{\Delta}_i \sin\theta_i) + u_{o_j}' \frac{\bar{\Delta}j}{2} \cos\theta_j + w_{o_j}' \frac{\bar{\Delta}j}{2} \sin\theta_j \; ; \tag{A.24}$$

on lower surface

$$\phi_{o_j} = \sum_{i=j-1}^{N/2} (u_{o_i}' \bar{\Delta}_i \cos\theta_i + w_{o_i}' \bar{\Delta}_i \sin\theta_i) + u_{o_j}' \frac{\bar{\Delta}_j}{2} \cos\theta_j + w_{o_j}' \frac{\bar{\Delta}_j}{2} \sin\theta_j \; .$$

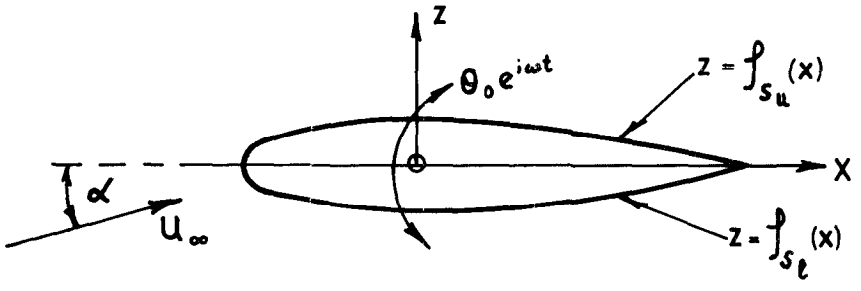

NOTATION FOR OSCILLATING AEROFOIL

Fig. 1

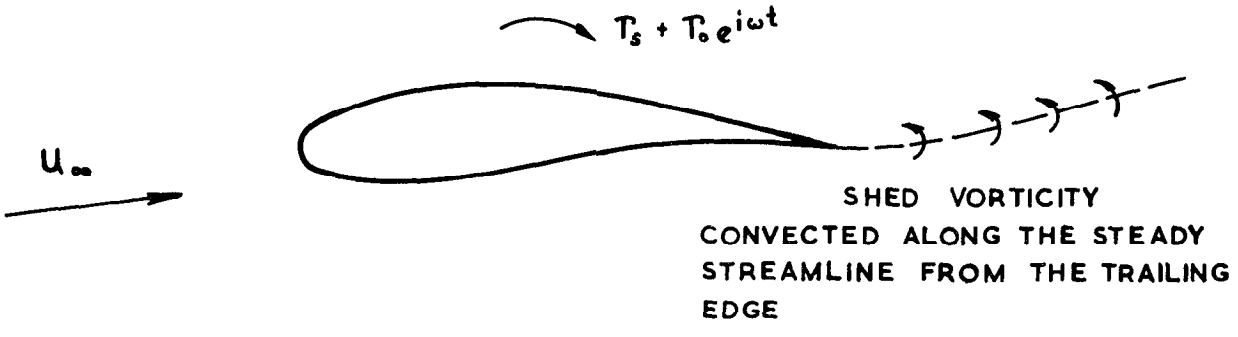

WAKE MODEL

Fig. 2

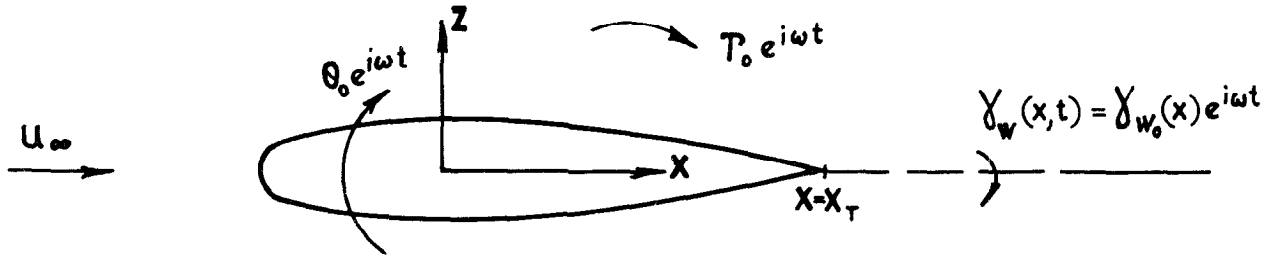

SYMMETRICAL AEROFOIL AT 0° INCIDENCE AND THE TRAILING VORTEX SHEET

Fig. 3

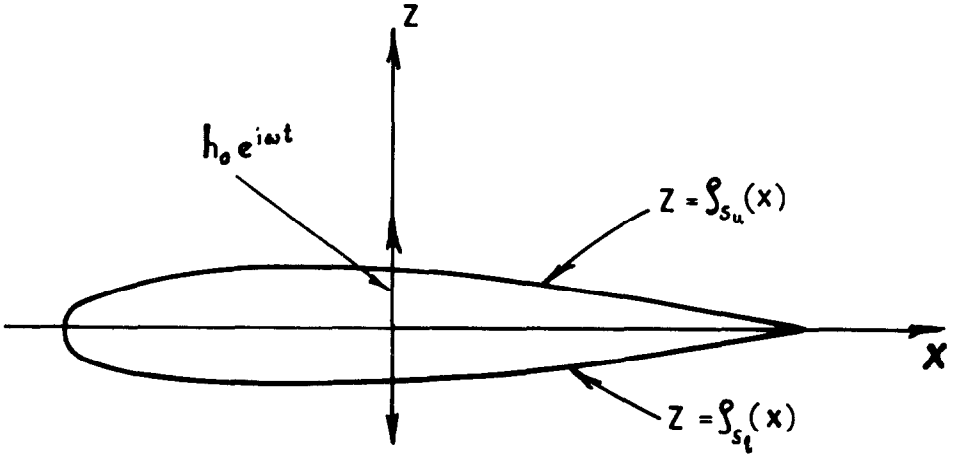

NOTATION FOR HEAVING OSCILLATION

Fig. 4

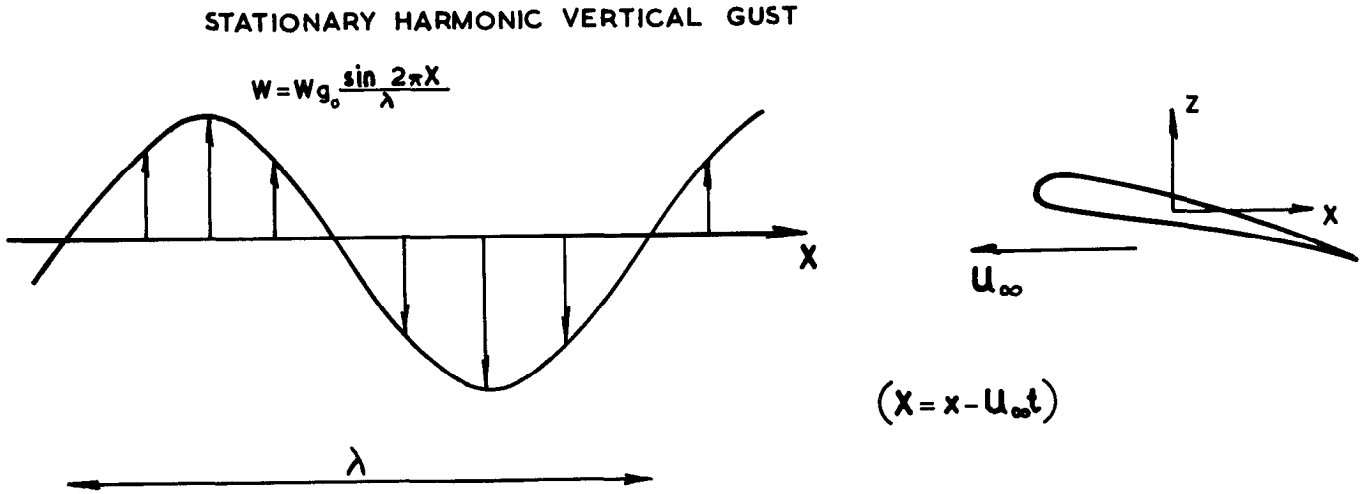

MOTION IN STATIONARY VERTICAL SINUSOIDAL GUST

Fig. 5a.

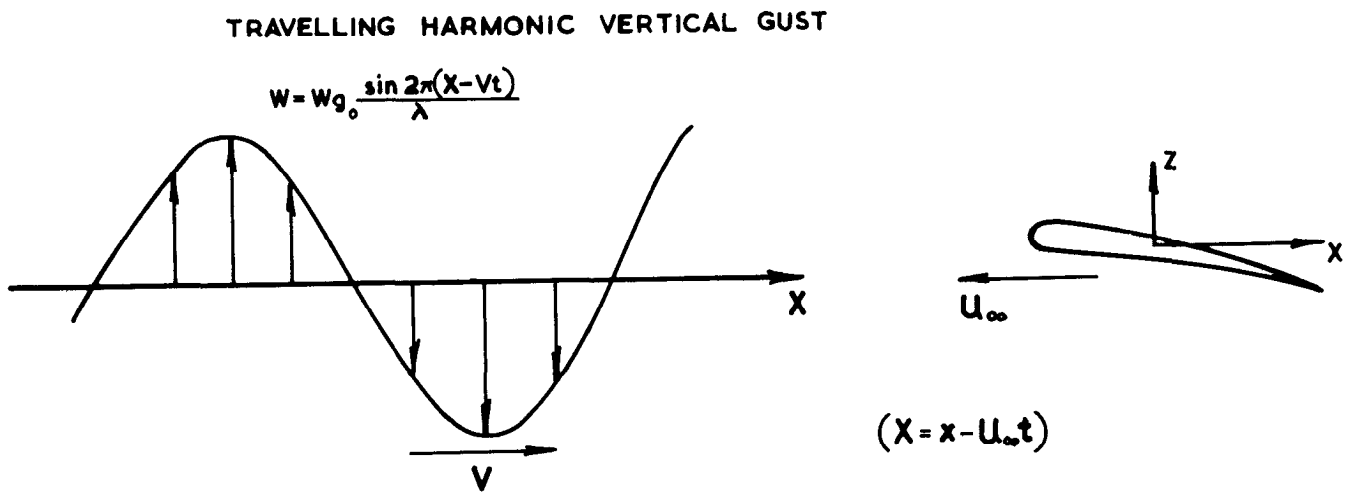

MOTION IN TRAVELLING VERTICAL SINUSOIDAL GUST

Fig. 5b.

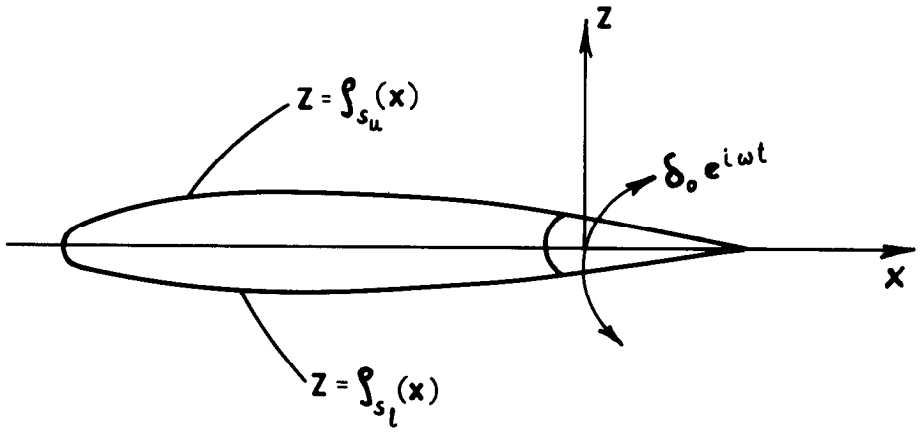

NOTATION FOR OSCILLATING CONTROL SURFACE

Fig. 6

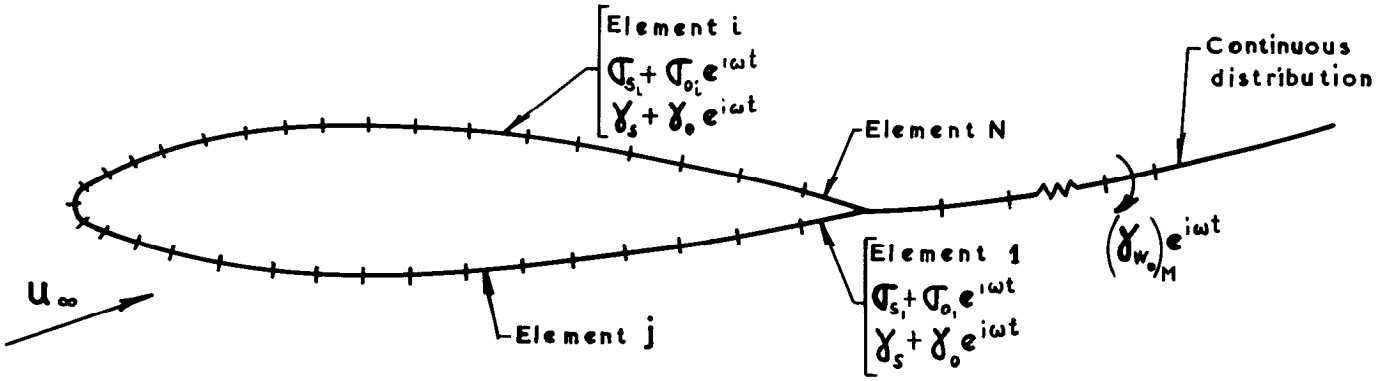

AEROFOIL AND THE WAKE REPRESENTED BY THE DISTRIBUTION OF SOURCES AND VORTICITY

Fig. 7

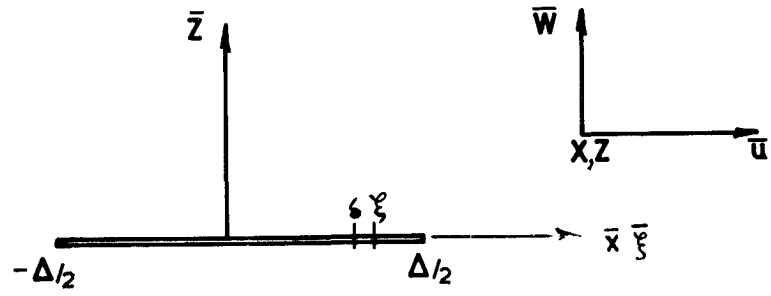

SOURCE ELEMENT

Fig. 8 a.

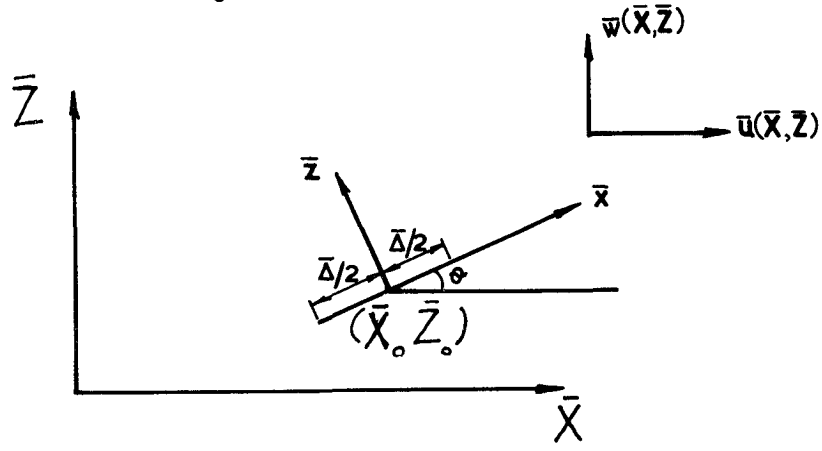

AXES SYSTEM

Fig. 8 b.

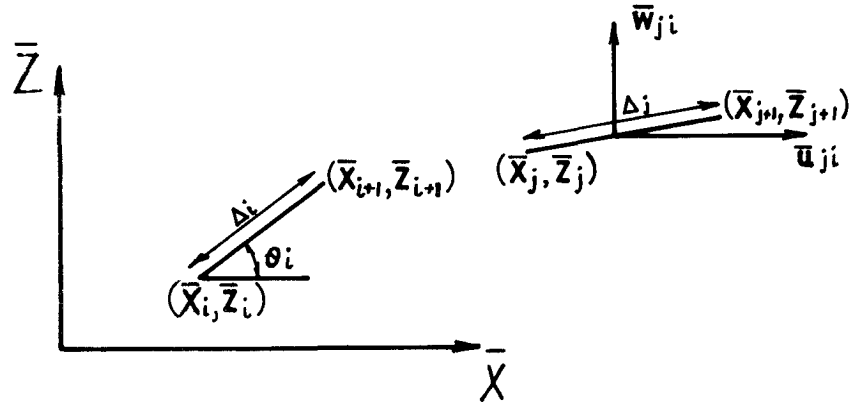

ORIENTATION OF i^{th} ELEMENT IN RELATION TO j^{th} ELEMENT

Fig. 8 c.

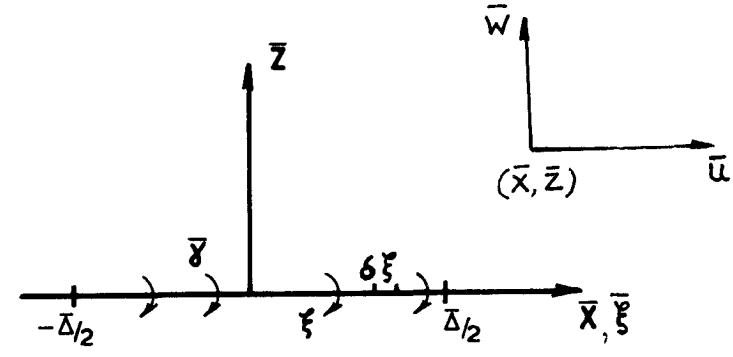

VORTICITY DISTRIBUTION ON AN ELEMENT

Fig. 9

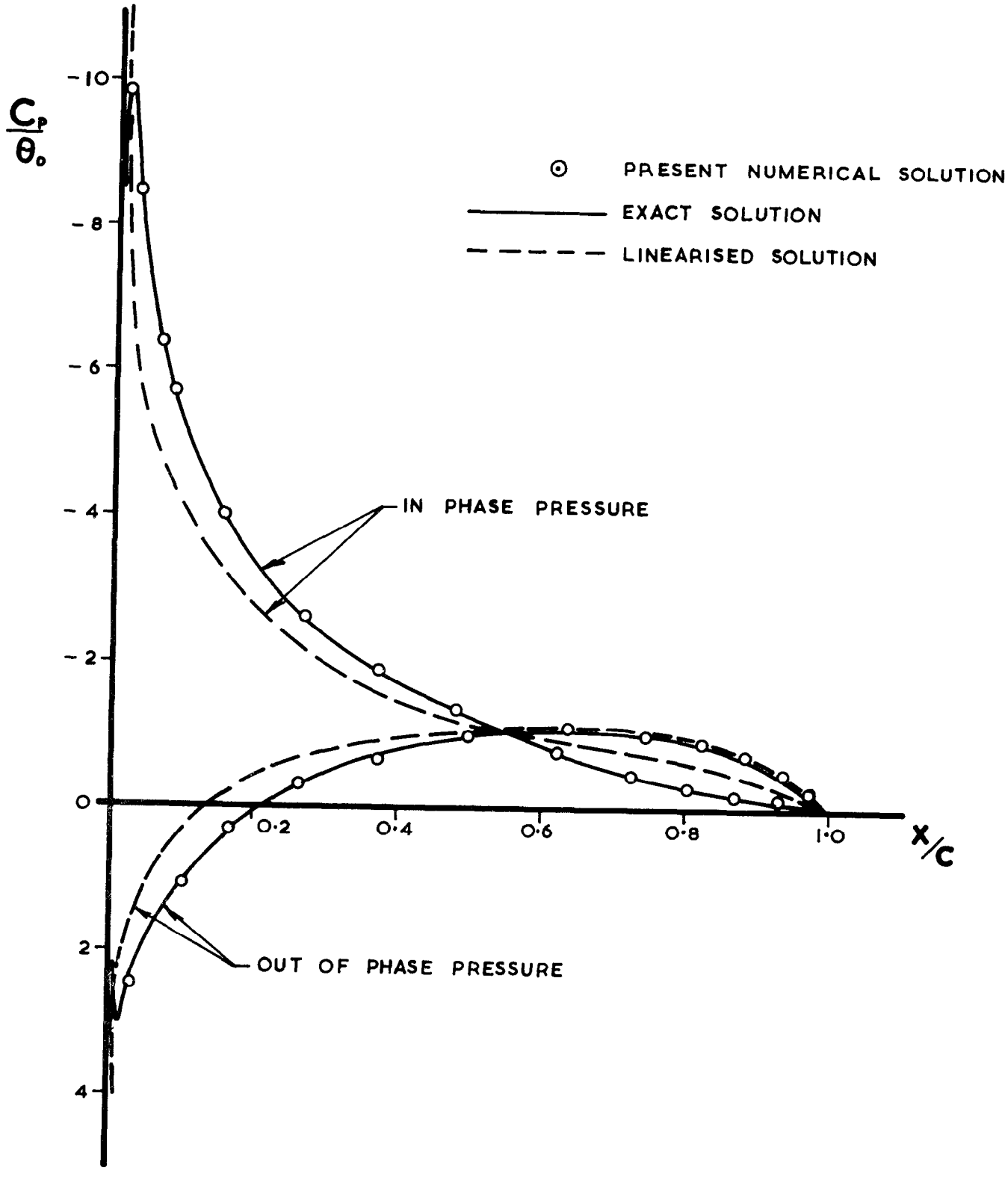

DE VOOREN-VEL AEROFOIL OSCILLATING ABOUT MID-CHORD POSITION

MEAN ANGLE OF INCIDENCE 0°
FREQUENCY PARAMETER γ 0·8

Fig. 10

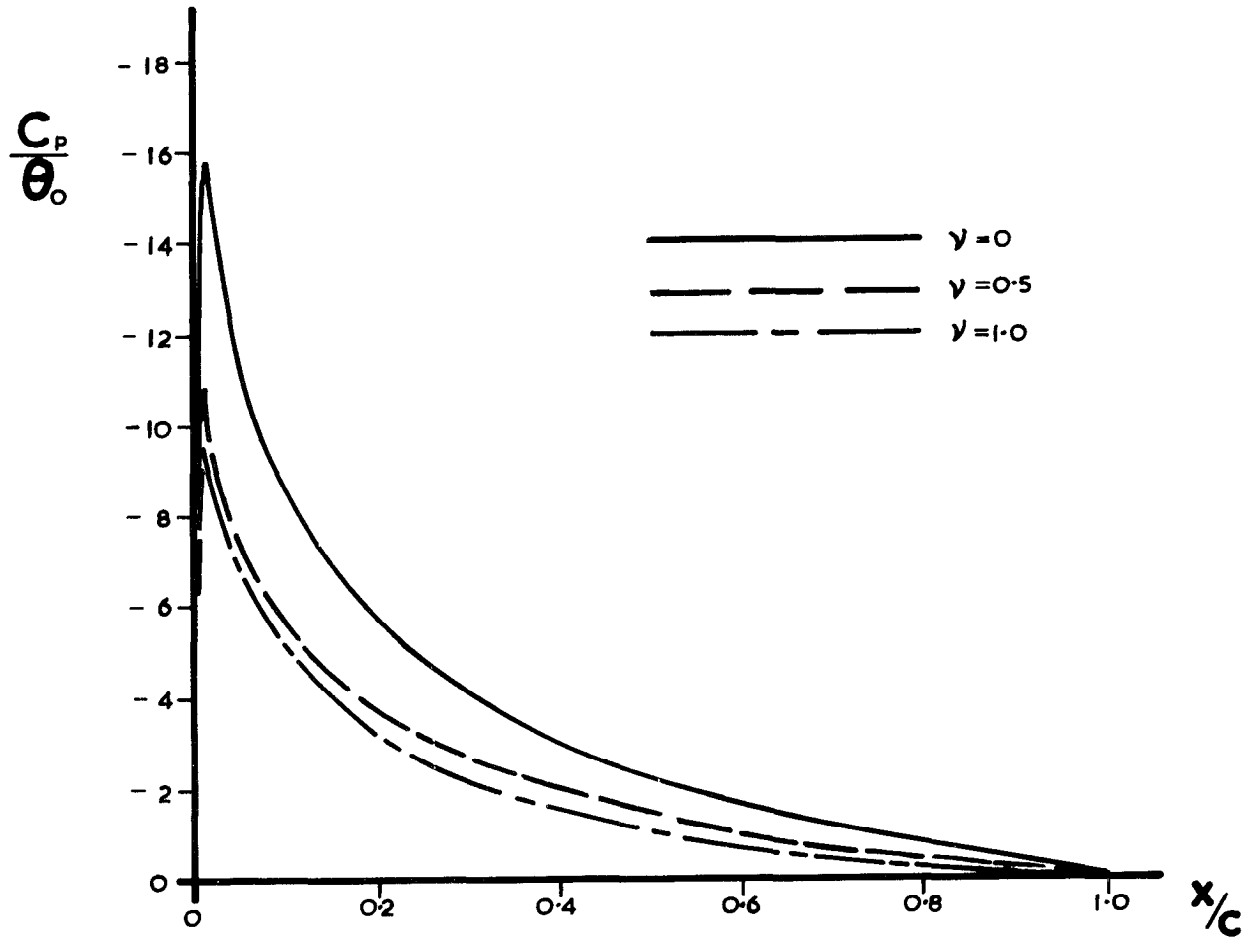

IN PHASE PRESSURE DISTRIBUTION

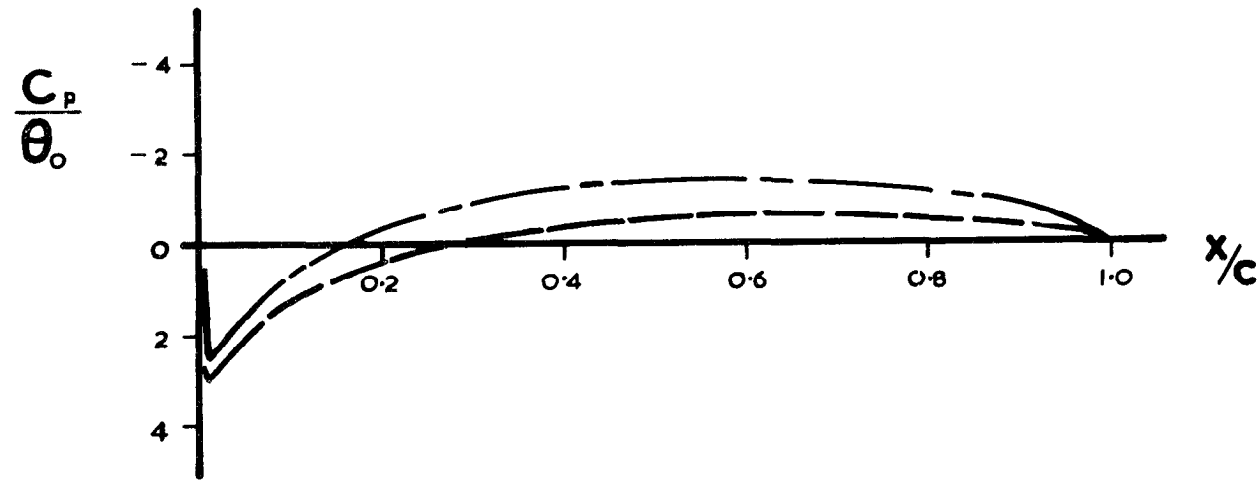

OUT OF PHASE PRESSURE DISTRIBUTION

DE VOOREN-VEL AEROFOIL OSCILLATING
ABOUT MID CHORD POSITION
MEAN ANGLE OF INCIDENCE 0°

Fig. 11

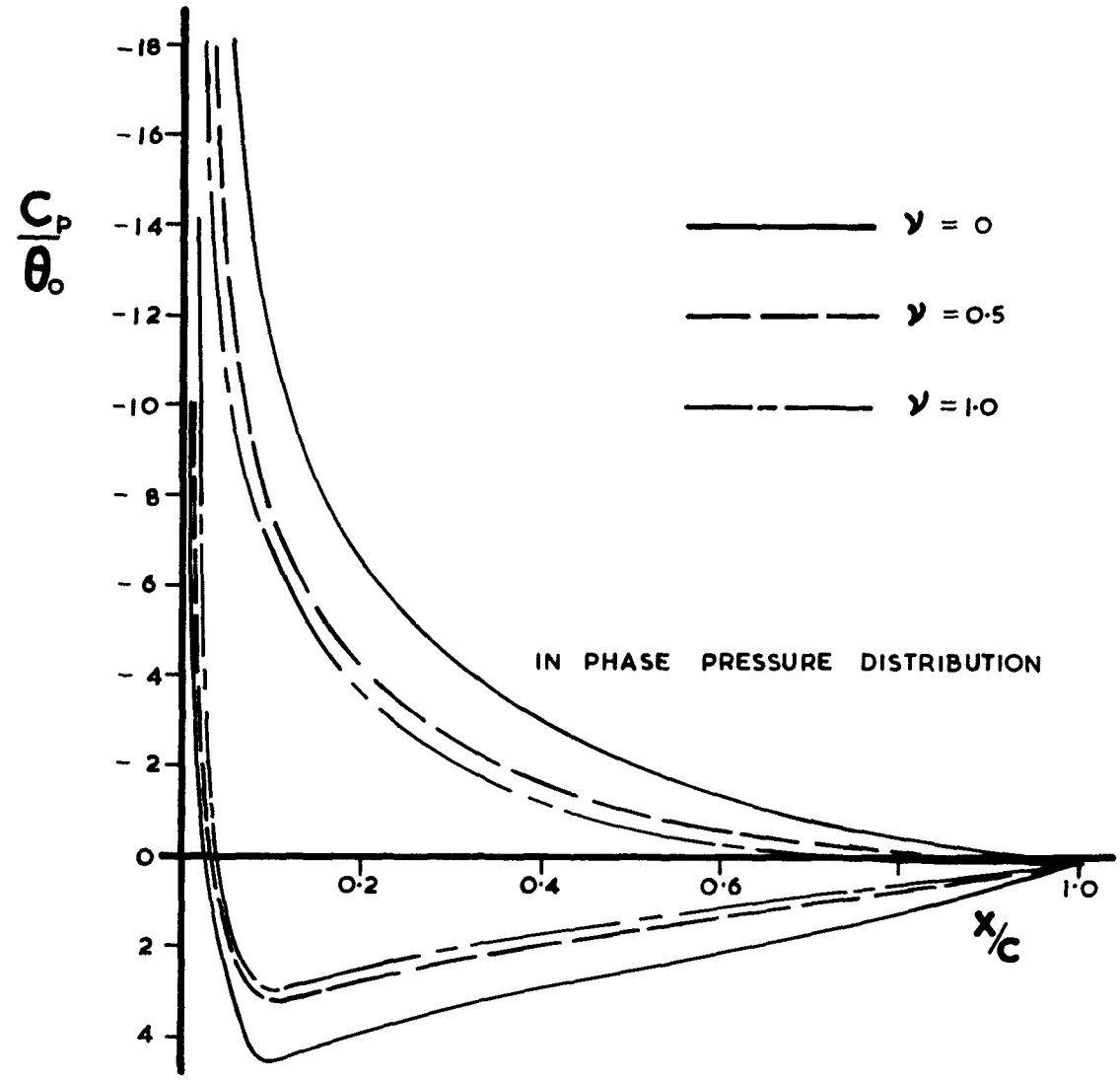

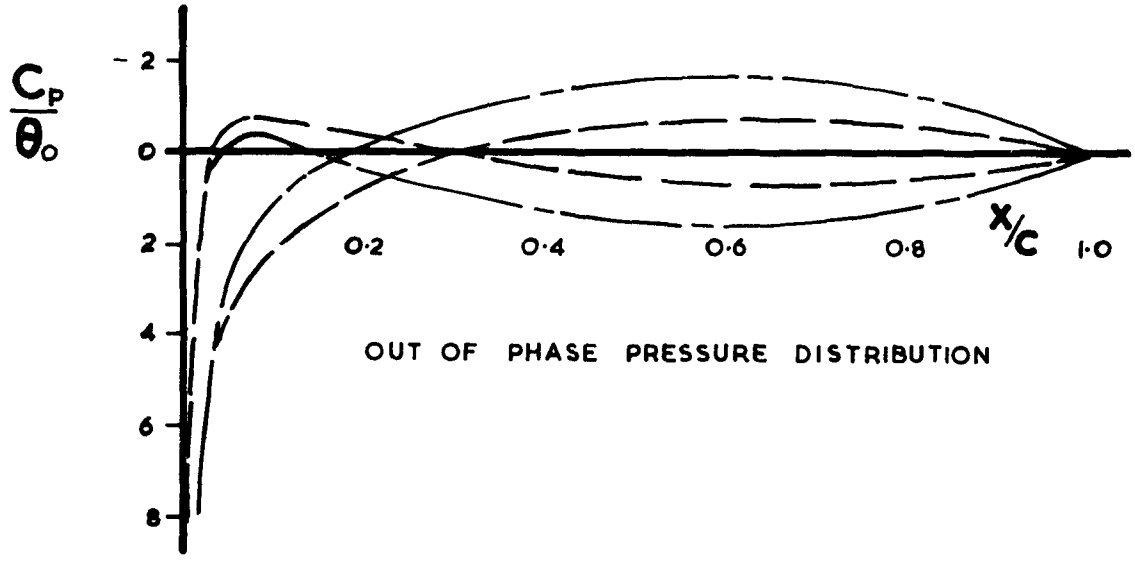

VAN DE VOOREN AEROFOIL

OSCILLATING ABOUT MID-CHORD POSITION
MEAN ANGLE OF INCIDENCE 10°

Fig. 12(a)

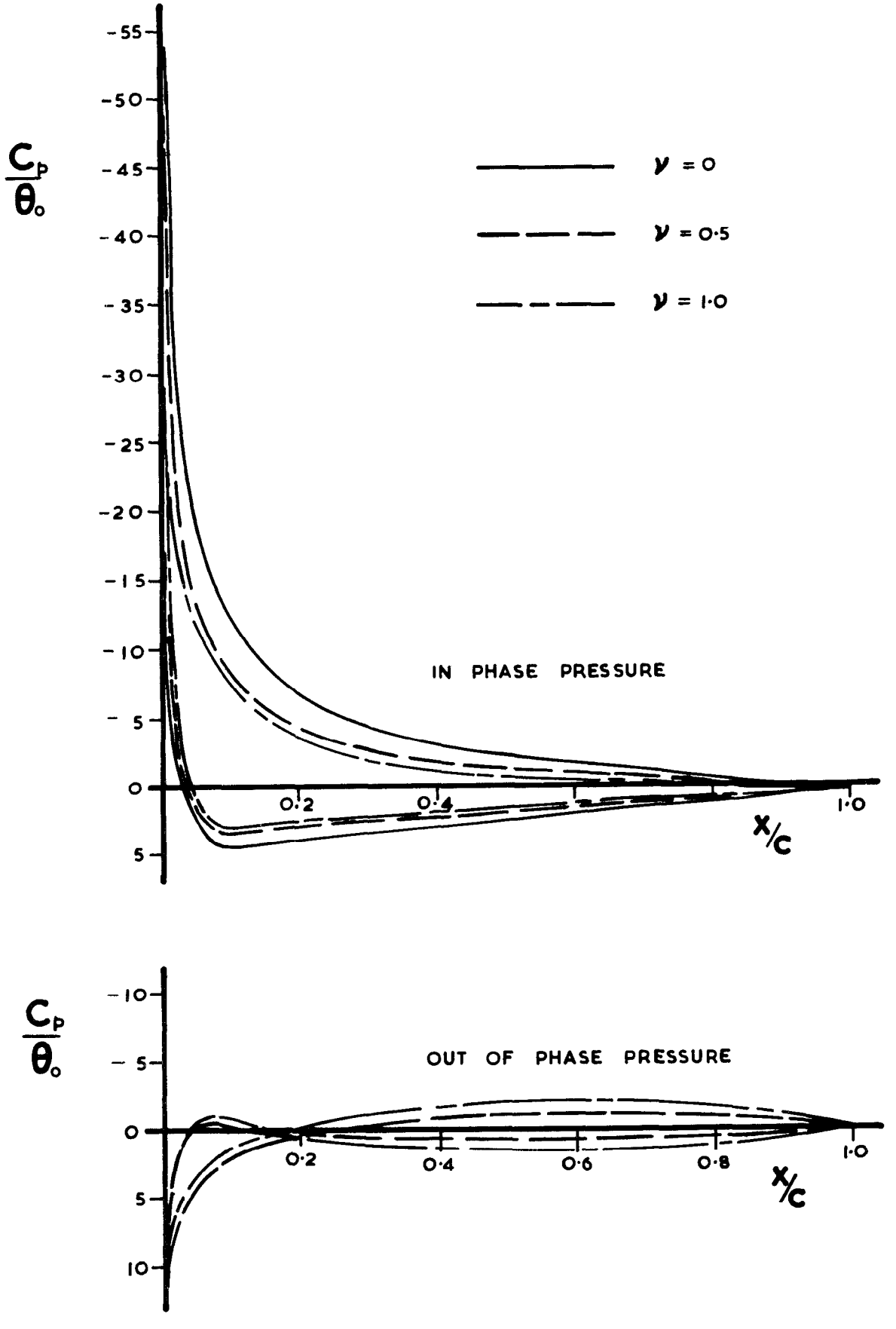

DE VOOREN-VEL AEROFOIL

OSCILLATING ABOUT MID-CHORD POSITION

MEAN ANGLE OF INCIDENCE 10°

Fig. 12(b)

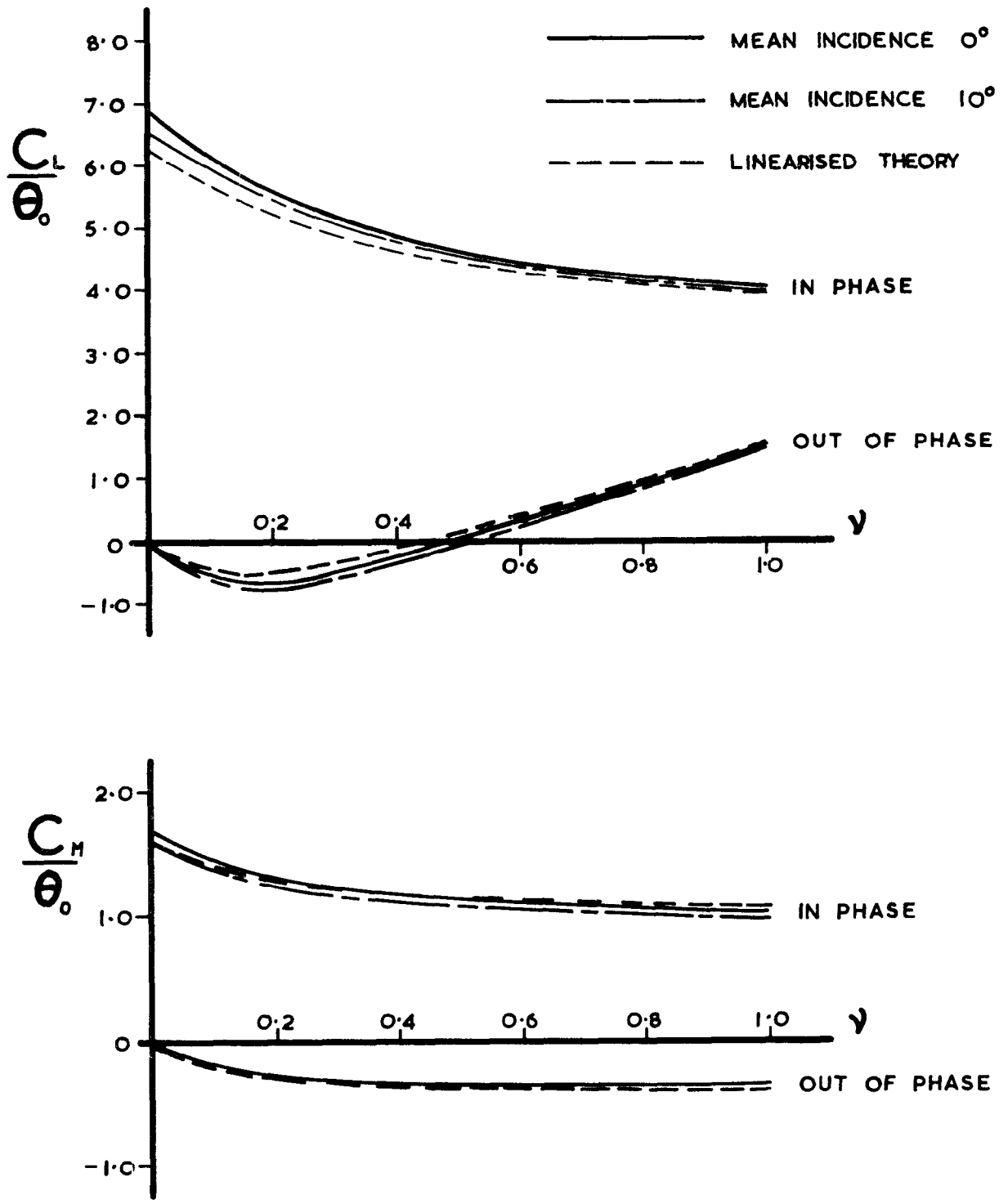

Symmetrical Karman–Trefftz aerofoil oscillating about mid-chord position

Fig. 13

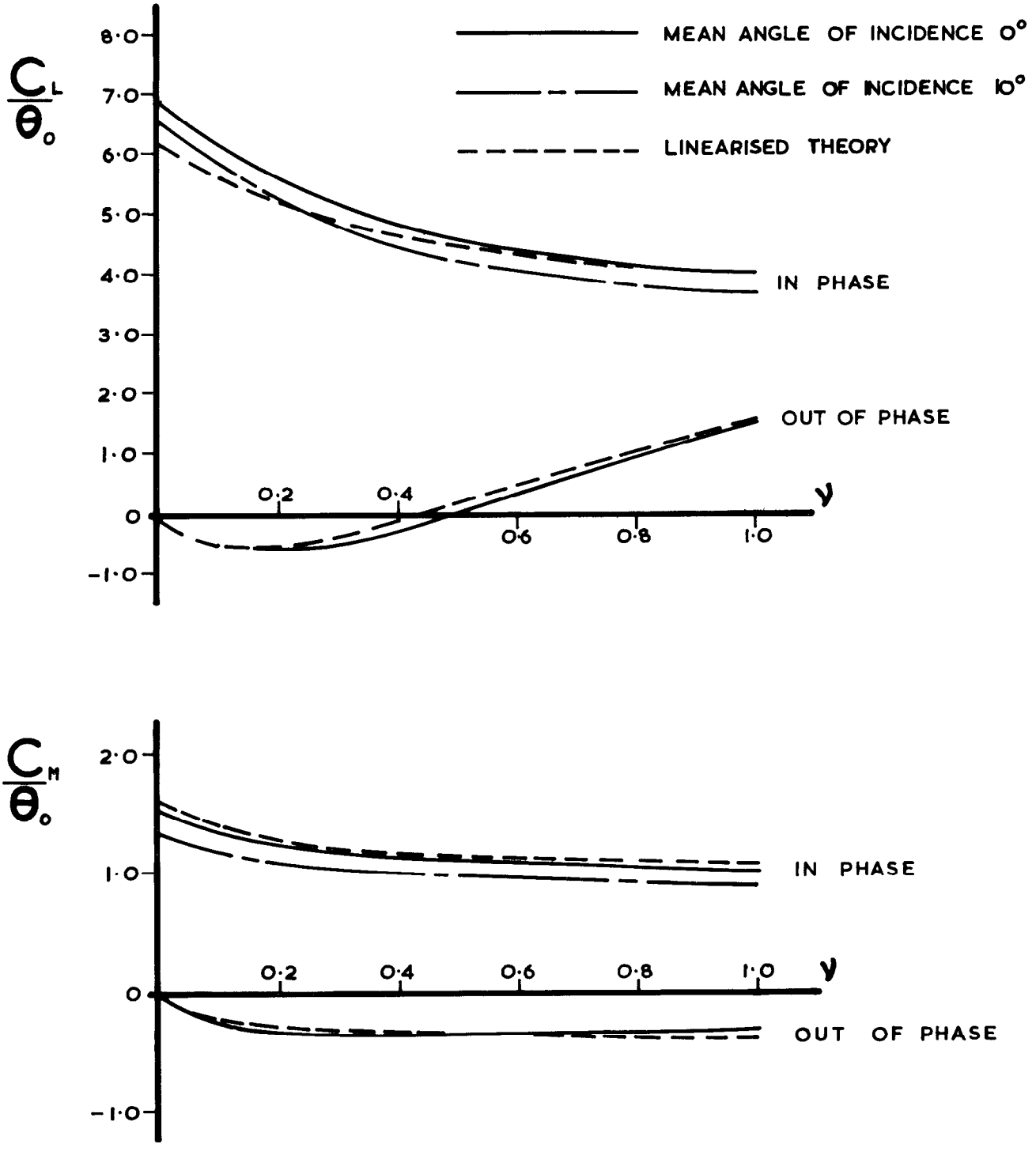

Karman-Trefftz aerofoil (8·6 % camber) oscillating about mid-chord position

Fig. 14

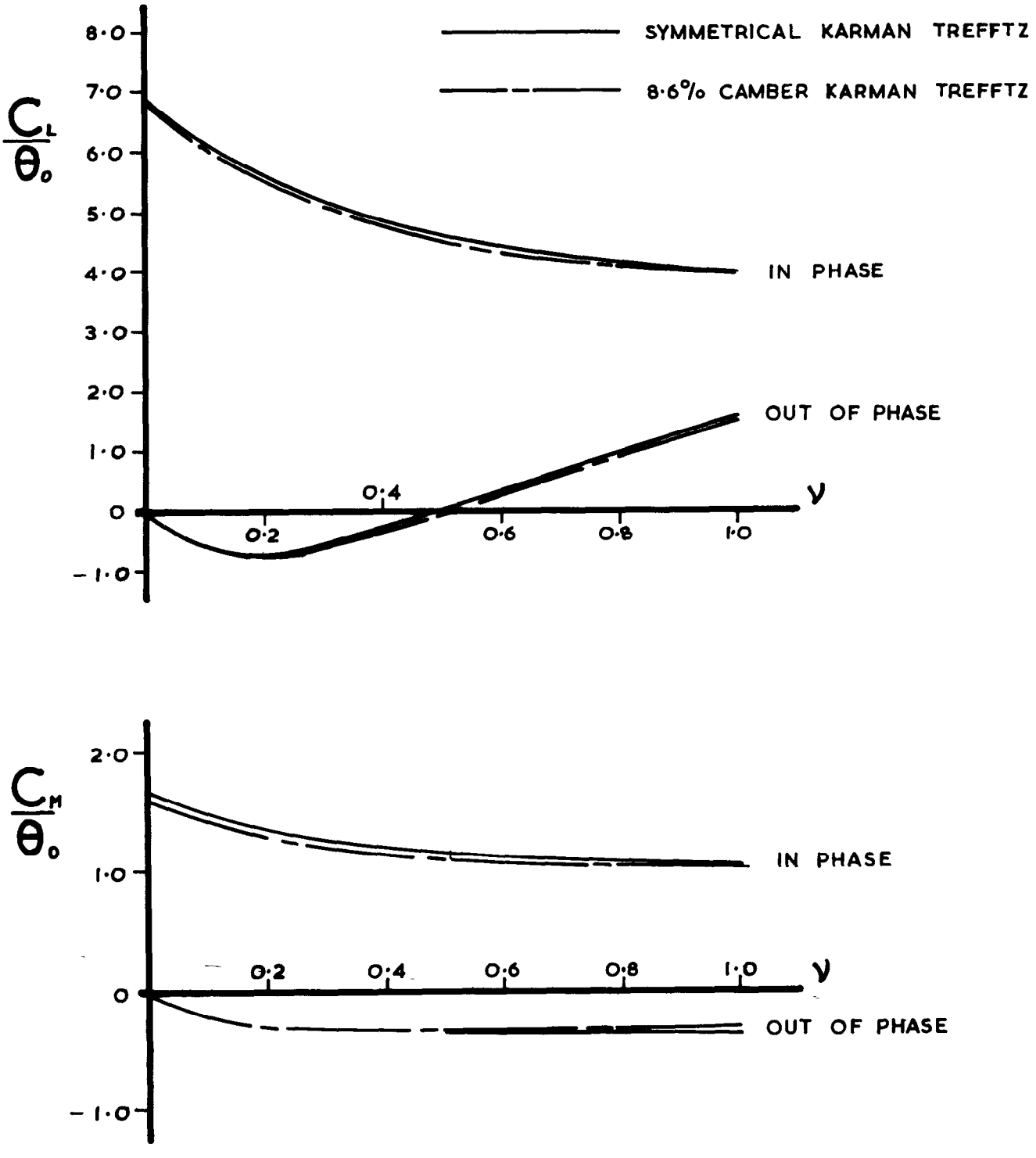

Effect of camber
Mean angle of incidence 0°

Fig. 15 (a)

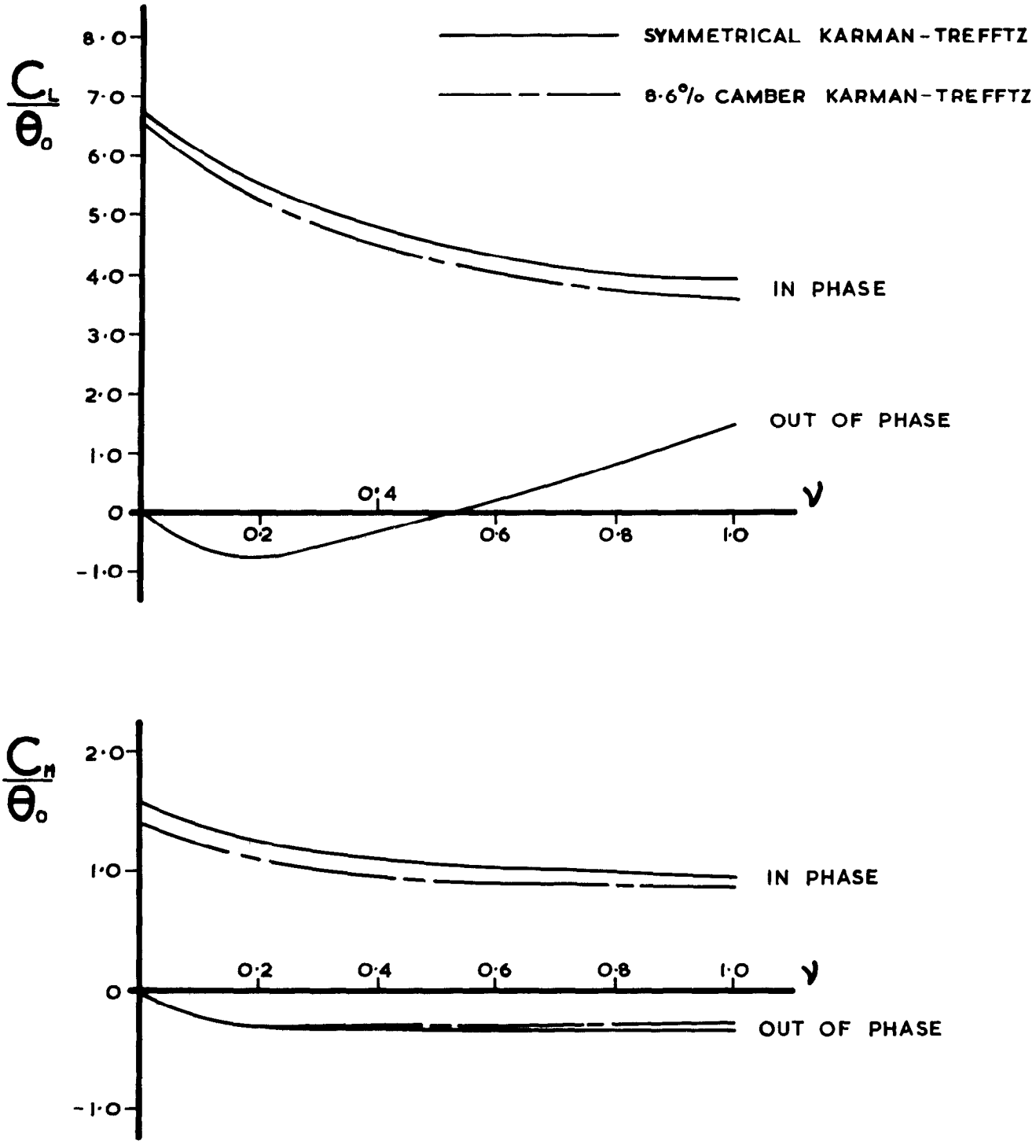

Effect of camber

Mean angle of incidence 10°

Fig. 15 (b)

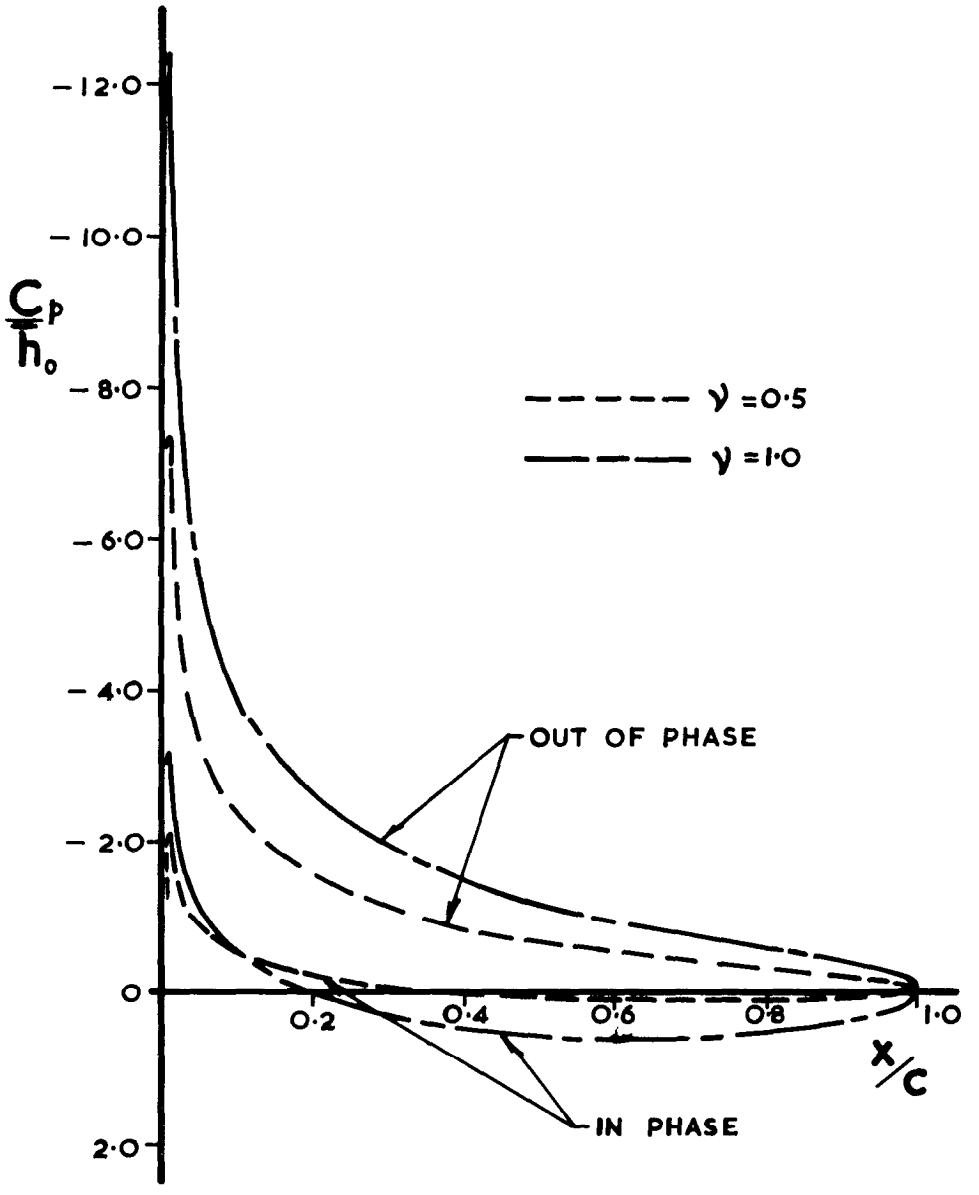

8·4 % THICK SYMMETRICAL VON MISES AEROFOIL HEAVING OSCILLATION AT 0° INCIDENCE

Fig. 16

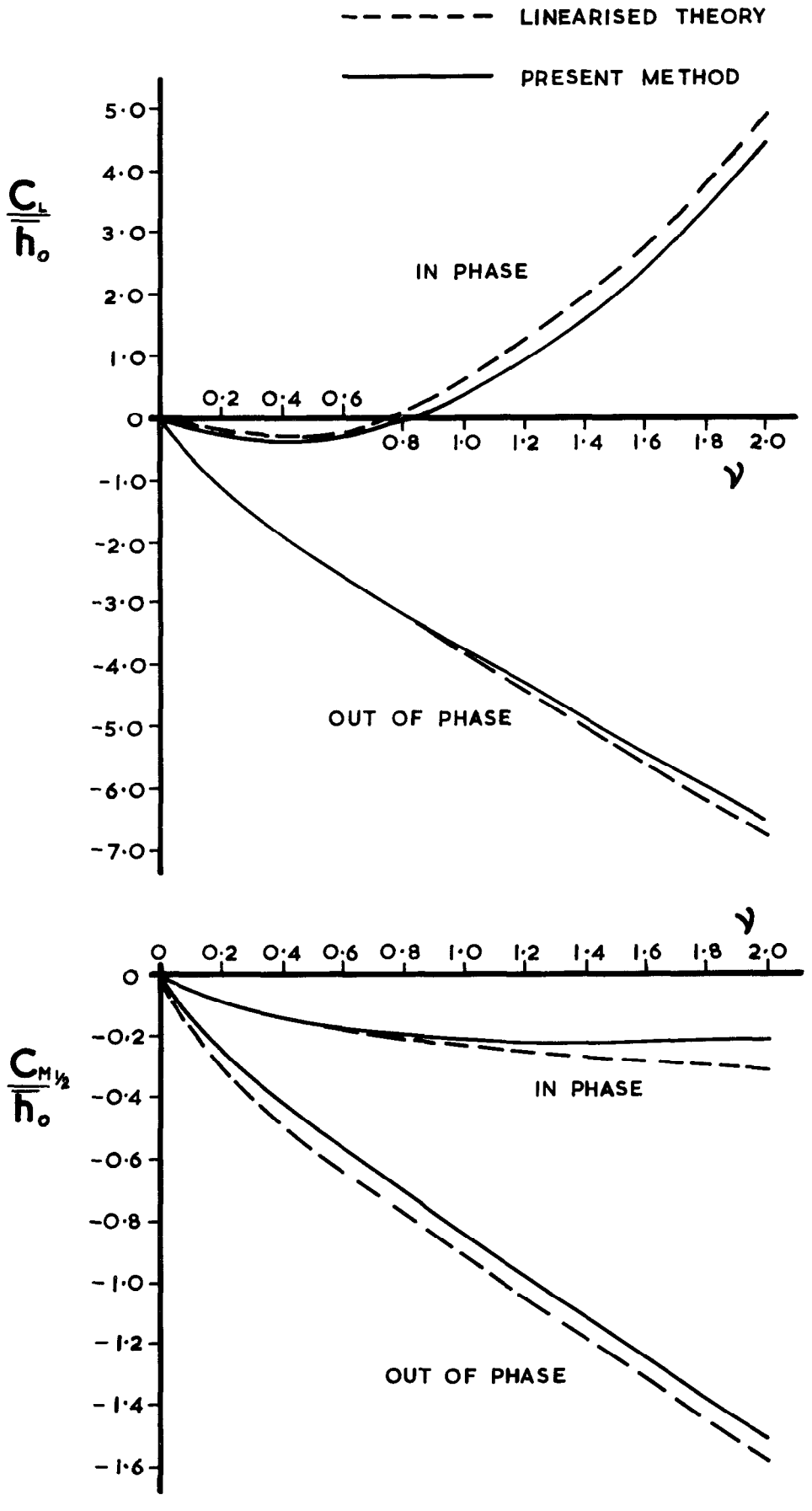

8·4 % THICK SYMMETRICAL VON MISES AEROFOIL

HEAVING OSCILLATION AT 0° INCIDENCE

Fig. 17

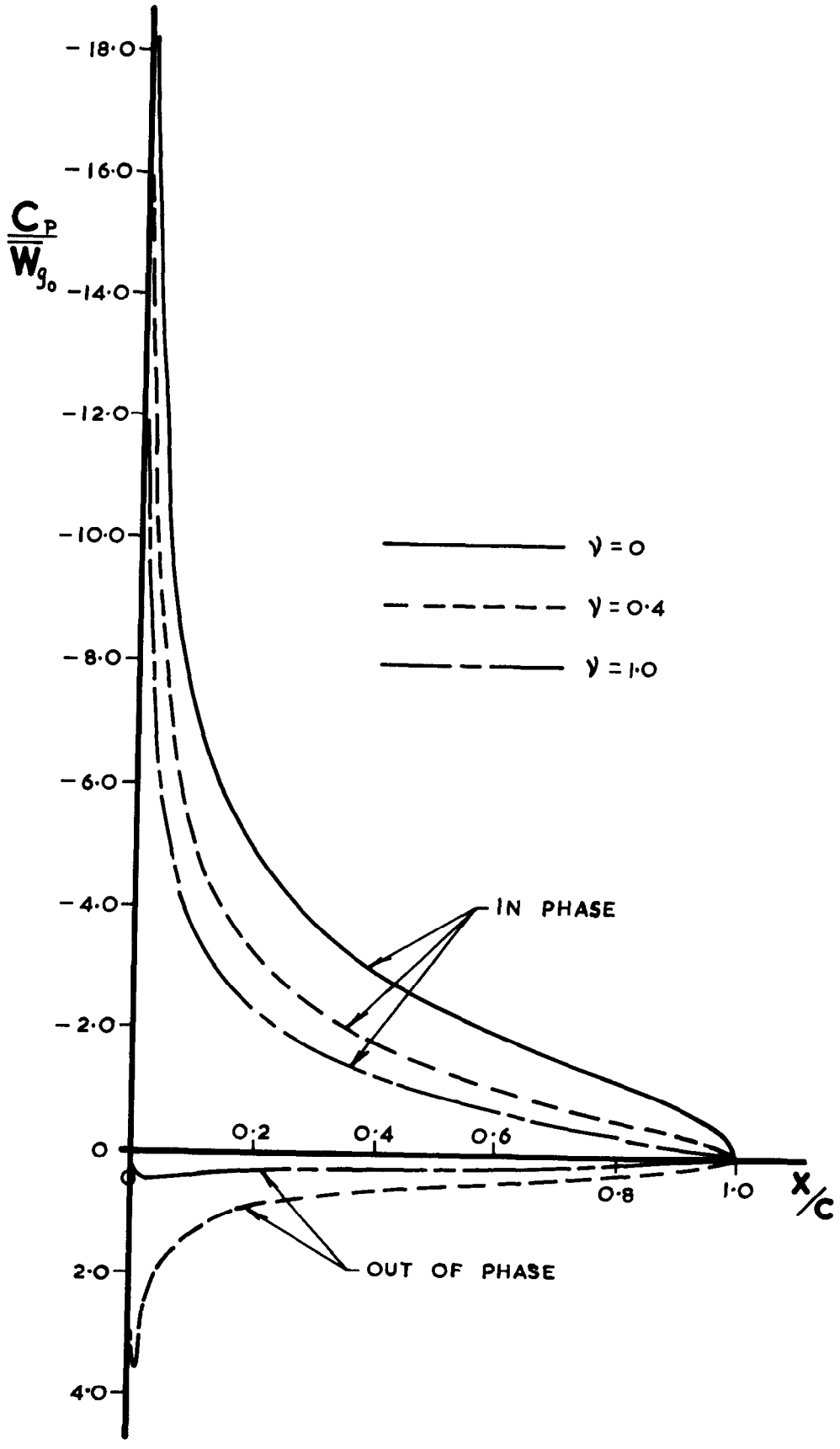

8·4% THICK SYMMETRICAL VON MISES AEROFOIL

SINUSOIDAL GUST RESPONSE AT 0° INCIDENCE

Fig. 18

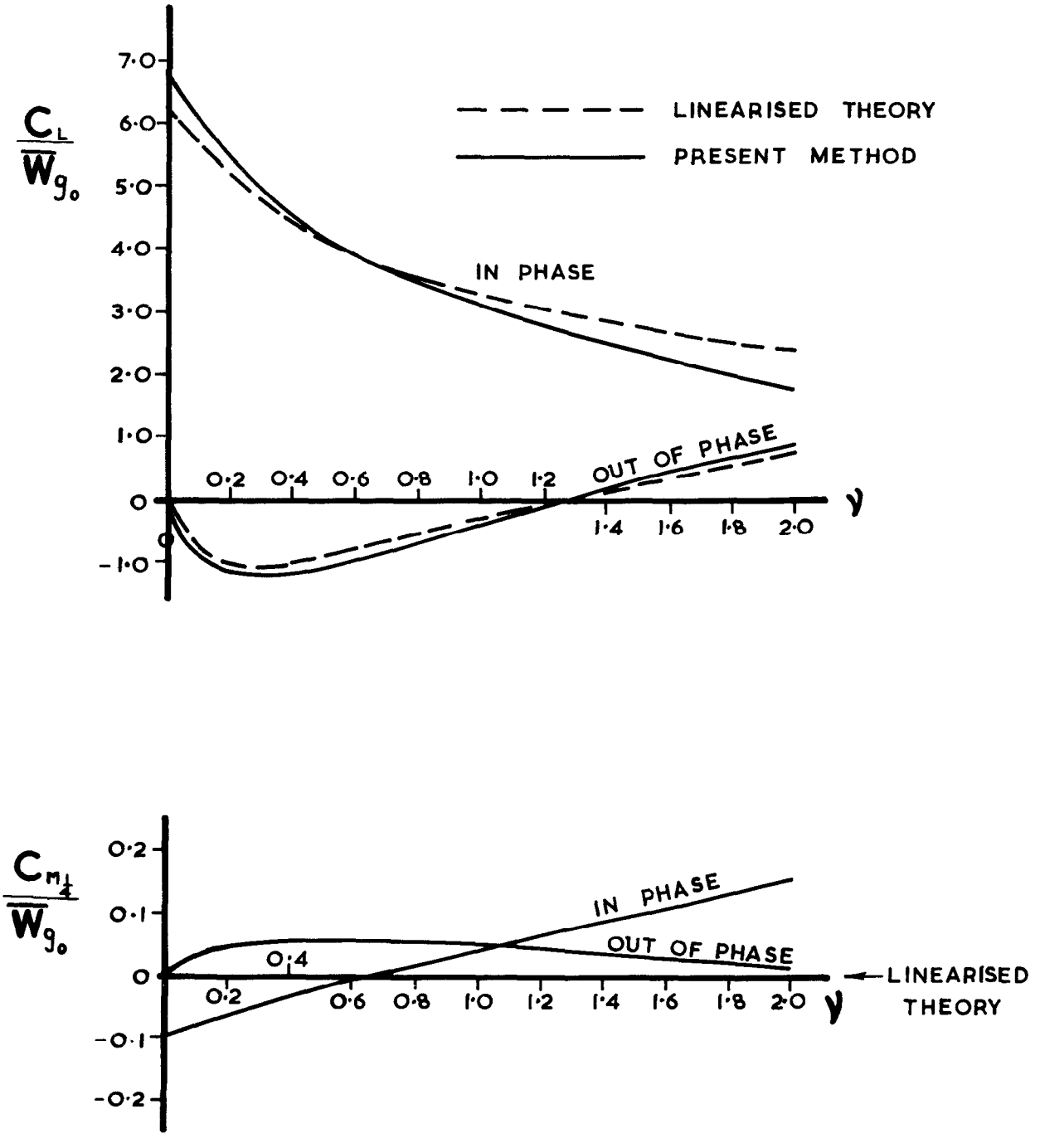

8·4 % THICK SYMMETRICAL VON MISES AEROFOIL

SINUSOIDAL GUST RESPONSE AT 0° INCIDENCE

Fig. 19

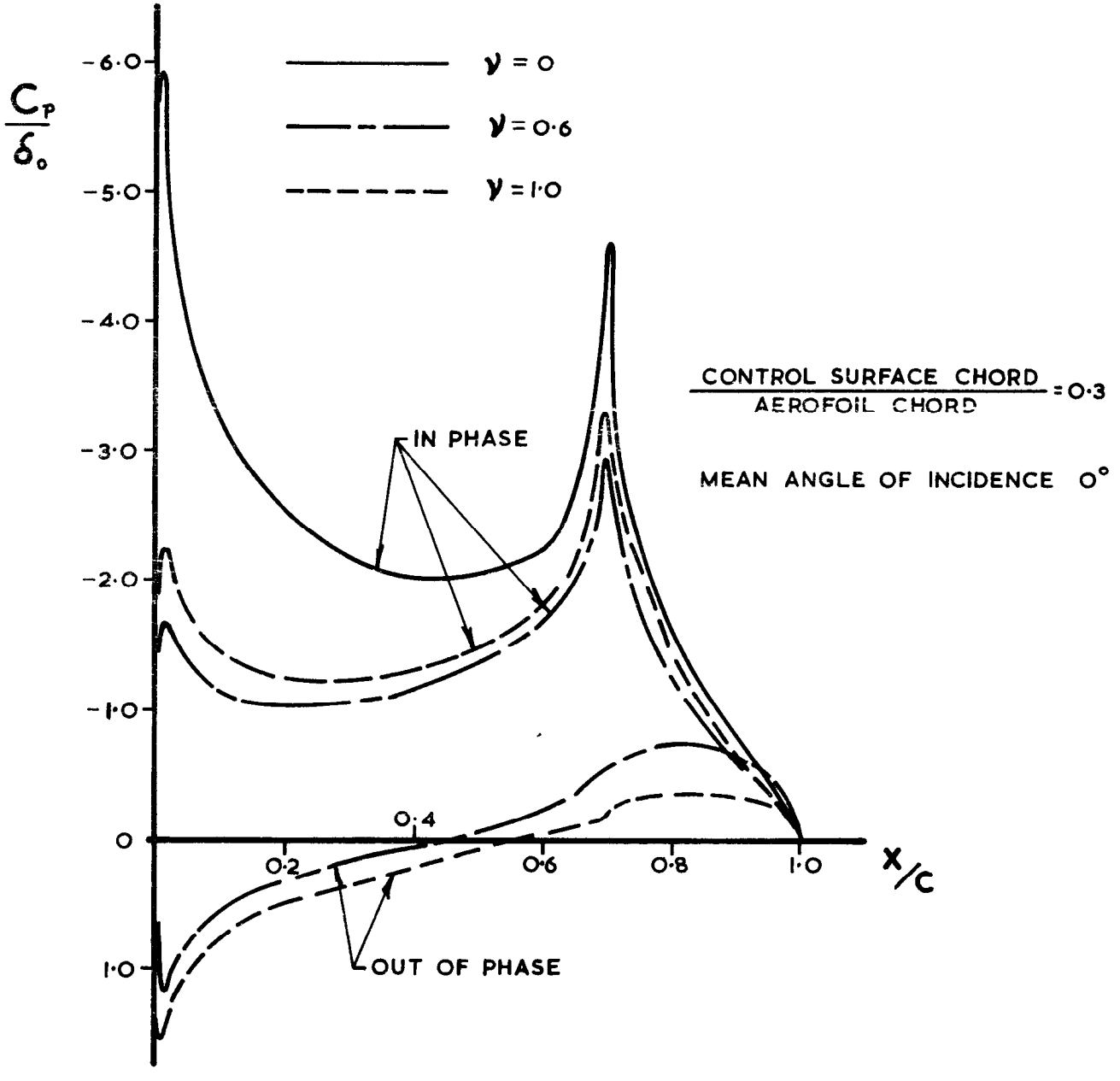

SYMMETRICAL KARMAN TREFFTZ AEROFOIL
WITH OSCILLATING CONTROL SURFACE

Fig. 20

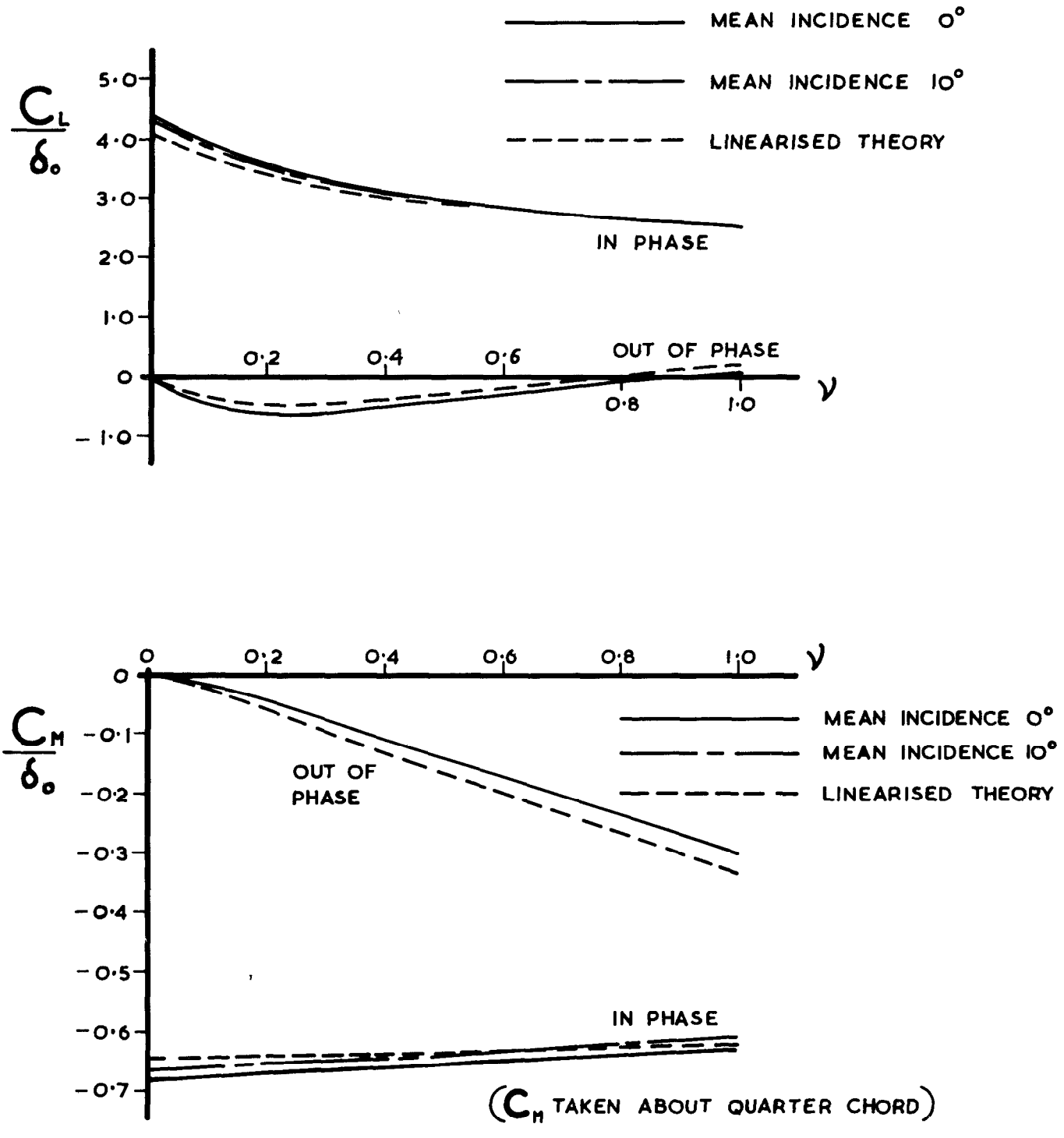

Symmetrical Karman-Trefftz aerofoil with oscillating control surface

$$\frac{\text{CONTROL SURFACE CHORD}}{\text{AEROFOIL CHORD}} = 0.3$$

Fig. 21 (a)

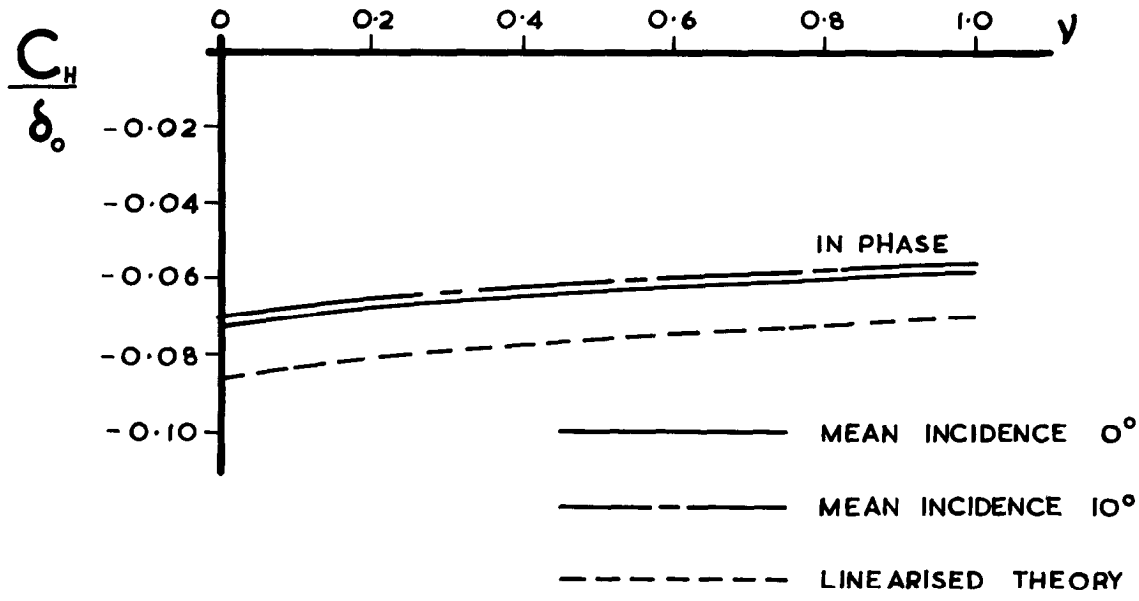

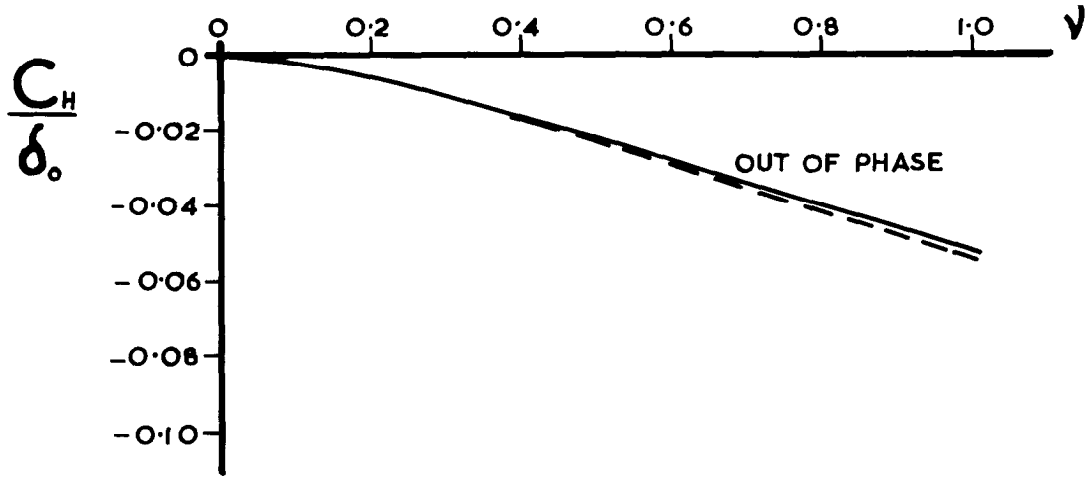

Symmetrical Karman-Trefftz aerofoil with oscillating control surface

$$\frac{\text{CONTROL SURFACE CHORD}}{\text{AEROFOIL CHORD}} = 0{\cdot}3$$

Fig. 21(b)

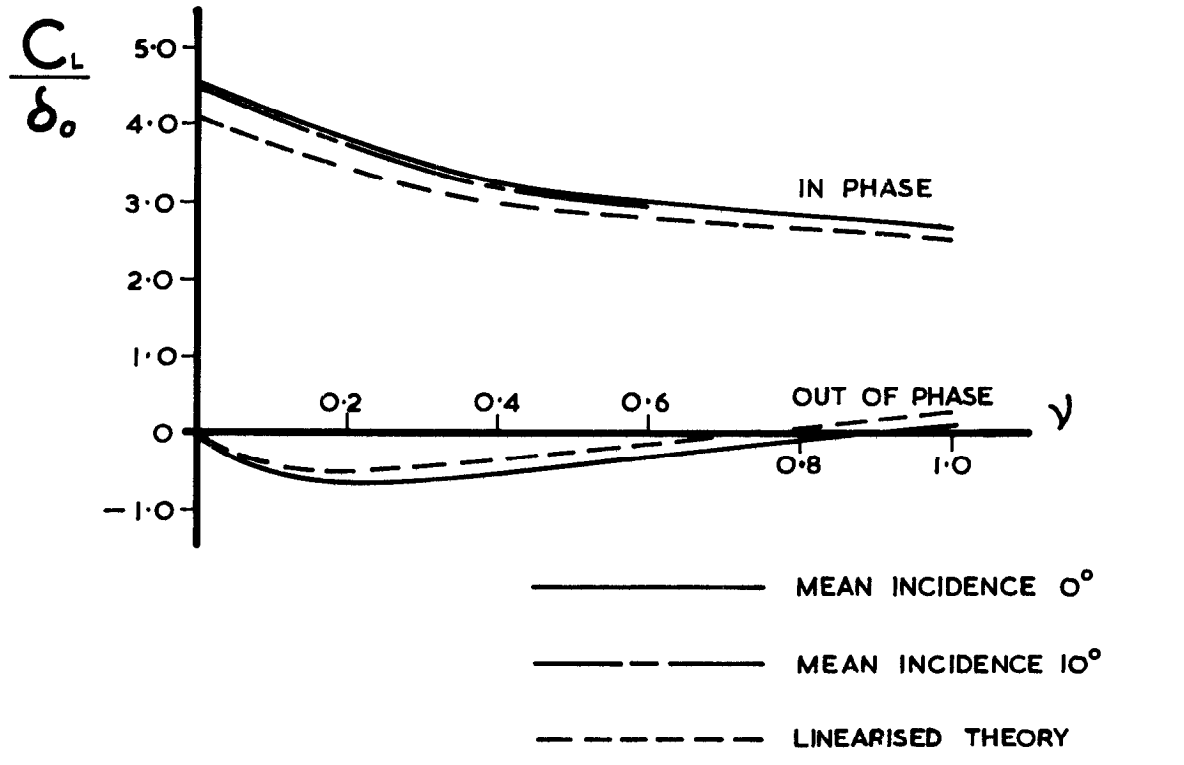

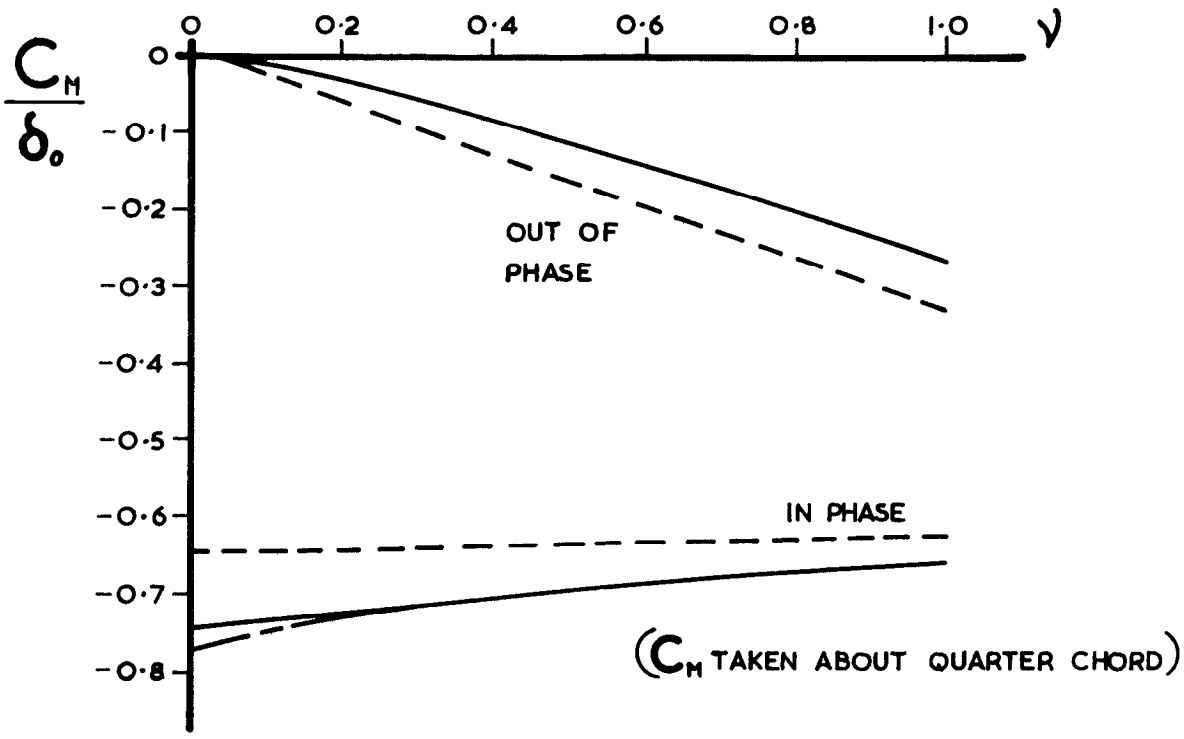

Karman-Trefftz aerofoil (8·6% camber) with oscillating control surface

$$\frac{\text{CONTROL SURFACE CHORD}}{\text{AEROFOIL CHORD}} = 0{\cdot}3$$

Fig. 22(a)

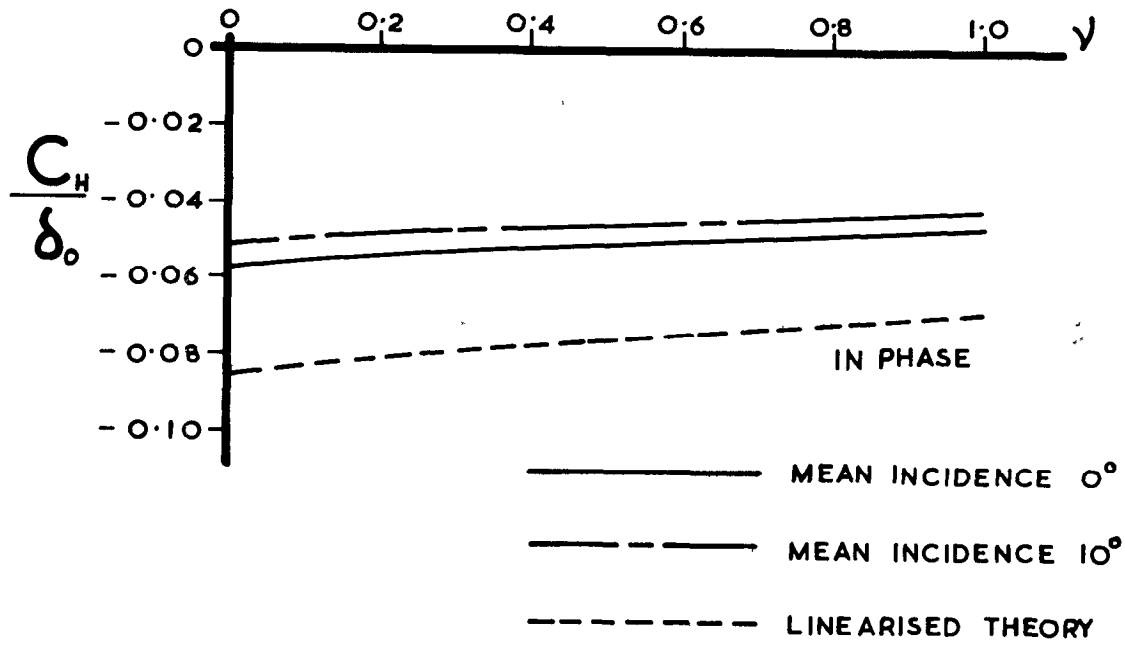

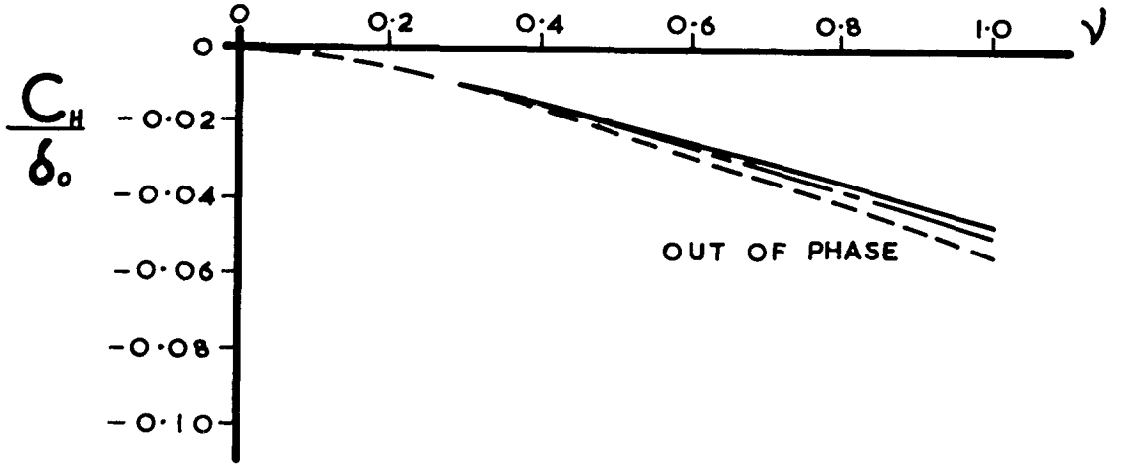

Karman–Trefftz aerofoil (8·6% camber) with oscillating control surface

$$\frac{\text{CONTROL SURFACE CHORD}}{\text{AEROFOIL CHORD}} = 0{\cdot}3$$

Fig. 22(b)

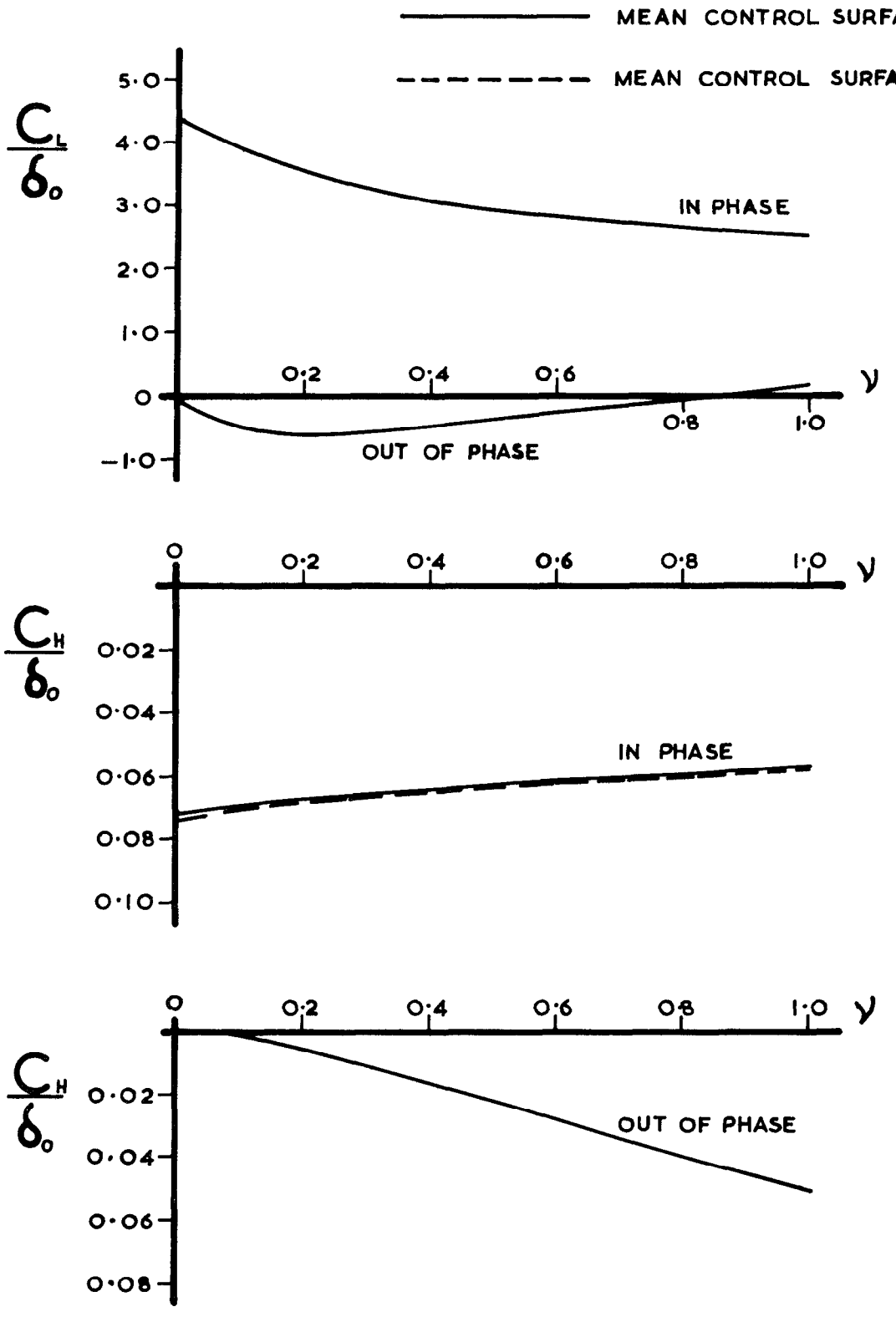

Effect of control surface mean incidence

Fig. 23

Produced in England by Her Majesty's Stationery Office, Reprographic Centre, Basildon

Bas 45231/587483 K4 2/78 P

ARC CP No.1392
September 1976
Basu, B.C. and Hancock, G.J.

TWO-DIMENSIONAL AEROFOILS AND CONTROL SURFACES IN SIMPLE HARMONIC MOTION IN INCOMPRESSIBLE INVISCID FLOW

A numerical method based on the A.M.O. Smith technique has been developed for the calculation of the two-dimensional potential flow about an aerofoil of arbitrary shape undergoing small amplitude simple harmonic motions. Problems considered include aerofoils oscillating in pitch, aerofoils oscillating in heave, aerofoils in harmonic travelling gusts and control surface oscillations. Comparison with analytic solutions, where available, is good.

ARC CP No.1392
September 1976
Basu, B.C. and Hancock, G.J.

TWO-DIMENSIONAL AEROFOILS AND CONTROL SURFACES IN SIMPLE HARMONIC MOTION IN INCOMPRESSIBLE INVISCID FLOW

A numerical method based on the A.M.O. Smith technique has been developed for the calculation of the two-dimensional potential flow about an aerofoil of arbitrary shape undergoing small amplitude simple harmonic motions. Problems considered include aerofoils oscillating in pitch, aerofoils oscillating in heave, aerofoils in harmonic travelling gusts and control surface oscillations. Comparison with analytic solutions, where available, is good.

ARC CP No.1392
September 1976
Basu, B.C. and Hancock, G.J.

TWO-DIMENSIONAL AEROFOILS AND CONTROL SURFACES IN SIMPLE HARMONIC MOTION IN INCOMPRESSIBLE INVISCID FLOW

A numerical method based on the A.M.O. Smith technique has been developed for the calculation of the two-dimensional potential flow about an aerofoil of arbitrary shape undergoing small amplitude simple harmonic motions. Problems considered include aerofoils oscillating in pitch, aerofoils oscillating in heave, aerofoils in harmonic travelling gusts and control surface oscillations. Comparison with analytic solutions, where available, is good.

ARC CP No.1392
September 1976
Basu, B.C. and Hancock, G.J.

TWO-DIMENSIONAL AEROFOILS AND CONTROL SURFACES IN SIMPLE HARMONIC MOTION IN INCOMPRESSIBLE INVISCID FLOW

A numerical method based on the A.M.O. Smith technique has been developed for the calculation of the two-dimensional potential flow about an aerofoil of arbitrary shape undergoing small amplitude simple harmonic motions. Problems considered include aerofoils oscillating in pitch, aerofoils oscillating in heave, aerofoils in harmonic travelling gusts and control surface oscillations. Comparison with analytic solutions, where available, is good.

DETACHABLE ABSTRACT CARDS

Significant differences between linear and non-linear theory are shown especially for the in-phase hinge moment coefficients.	Significant differences between linear and non-linear theory are shown especially for the in-phase hinge moment coefficients.
Significant differences between linear and non-linear theory are shown especially for the in-phase hinge moment coefficients.	Significant differences between linear and non-linear theory are shown especially for the in-phase hinge moment coefficients.

HER MAJESTY'S STATIONERY OFFICE

Government Bookshops

49 High Holborn, London WC1V 6HB
13a Castle Street, Edinburgh EH2 3AR
41 The Hayes, Cardiff CF1 1JW
Brazennose Street, Manchester M60 8AS
Southey House, Wine Street, Bristol BS1 2BQ
258 Broad Street, Birmingham B1 2HE
80 Chichester Street, Belfast BT1 4JY

Government publications are also available through booksellers

C.P. No. 1392

ISBN 0 11 471138 0